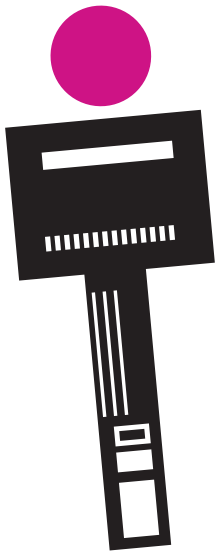

RAM ROBOTICS AND MECHATRONICS

SMART CONTROL OF MR SAFE PNEUMATIC STEPPER MOTORS

A.N. (Aniket) Singh

MSC ASSIGNMENT

Committee:
prof. dr. ir. L. Abelmann
dr. V. Groenhuis, MSc
dr. F.J. Siepel, MSc
prof. dr. ir. R.M. Verdaasdonk

April, 2021

017RaM2021
Robotics and Mechatronics
EEMCS
University of Twente
P.O. Box 217
7500 AE Enschede
The Netherlands

UNIVERSITY OF TWENTE. | TECHMED CENTRE UNIVERSITY OF TWENTE. | DIGITAL SOCIETY INSTITUTE

This page is intentionally left blank.

Summary

MRI-based invasive surgery requires that the equipments should be MR safe or MR conditional and does not interfere with the MRI scan. One such application is detection of lesion in breast that can only be detected on MRI. There are limitations in manual biopsy procedures, such as, the space inside the MRI scanner is not adequate for the radiologist to insert needle inside the scanner under visual guidance. While performing the procedure blindly outside the scanner may result in a failed biopsy. This can be overcome by using MR safe robotic system inside the scanner to increase accuracy and reduce the total time for the procedure.

The STORMRAM series and SUNRAM 5 are MR-safe robotic systems for breast biopsy, which uses pneumatic stepper motors and driven by feed-forward control algorithm. There are currently no sensors in the robots that makes calibration difficult and detection of missed steps impossible.

The objective of this thesis is to create a smart control of the pneumatic stepper motor for next-generation SUNRAM and related robotic systems. At the end of this thesis the new controller is able to apply features such as automatic calibration, position feedback system, higher speed and higher accuracy in comparison with previous controller.

Contents

List of Figures

List of Tables

Chapter 1

Introduction

Breast cancer is the most common cancer in women worldwide, with nearly 1.7 million new cases diagnosed in 2012, representing about 25% of all cancers in women. The superior sensitivity of magnetic resonance imaging (MRI) is reported to be as high as 94%–100%[3], thus it has been used for breast cancer screening and medical imaging by a radiologist to explore abnormalities. In this procedure, a biopsy needle is inserted to the location of the suspicious lesion under some imaging guidance after which the tissue is sampled and examined. While the larger lesions are well visible on other imaging techniques like X-ray and ultrasound but smaller lesions are only visible through MRI. The current MRI-guided breast biopsy is inaccurate and inefficient which results in long procedure times, additional tissue damage, and possibly a false negative biopsy[4].

This resulted in the development of several robotic systems which can be used inside an MRI scanner and allows precise needle operations under near-realtime MRI guidance which could improve the breast biopsy procedure. The construction and actuation method for this type of robot would require special consideration due to the MRI environment in which the robot needs to operate, making sure that using a robot inside an MRI scanner should not cause any interference with the imaging quality. In the current terminology as defined by the ASTM F2503-13 standard, three possible classifications are given to medical equipment: MR unsafe, MR conditional and MR safe. The strongest classification being MR safe is assigned to devices that are entirely constructed of materials that would not cause any interference with the imaging quality produced by the MRI scanner.

Since the robot actuates under an MRI environment, the energy source for actuation and sensor device cannot be electrical as it creates Radiofrequency (RF) interference which directly affects the MRI images being produced, this leads to actuation using mechanical energies such as pneumatic, hydraulic or cables. All three methods have their own advantages and disadvantages, but a major focus is given to the pneumatic system as it utilizes pressurized air as the medium which has the advantage that, it is abundant in hospitals, small leaks are acceptable as air is not hazardous and neither creates any sanitation problem even if it leaks. An important drawback is that air is compressible: while a single pneumatic cylinder could be used as an actuator, precise position control of the piston is difficult and the only well-defined positions are the two end-stop positions. This can be mitigated by using a stepper motor mechanism in which two or more pneumatic cylinders drive a rack or gear in discrete steps resulting in a pneumatic stepper motor [1].

1.1 Problem statement

The pneumatic stepper motors which are used by the different robotic systems have long pneumatic tubes in order to use the robot in MR safe conditions. The long pneumatic tubes that are connected with the robots cause pressure drop which results in low force output, this causes slipping, if the stepper motor is

operated at a high step frequency or high velocity. Due to this reason, the robotic system is operated at a slower speed in order to maintain position accuracy as there are currently no MR safe position sensors available for integration.

To improve the performance and reliability of the stepper motor there is a need for a *feedback system*. But the addition of the feedback system should not create any artifacts in the MR image. To tackle this problem, an MR safe optical encoder shall be developed, integrated, and tested in this thesis. Using this optical encoder, different control strategies shall be developed and tested. Currently, solenoid valves are widely used to send pneumatic signals to the stepper motor. In this thesis, its MR-safe alternative, a *pneumatic oscillator* shall also be tested. Further, a comparative study of performances of both solenoid driven system and pneumatic oscillator driven system shall be conducted.

The goal of this thesis is twofold: i) analysis of optical encoder system with a pneumatic stepper motor, thereby referring it as *smart pneumatic stepper motor*, and ii) analysis of driving a smart pneumatic stepper motor with *pneumatic oscillator*. These goals are then transformed into research questions which are:

1. What are the advantages and disadvantages of adding an optical encoder in a Pneumatic stepper motor?
    - How to implement an optical encoder in an MRI environment?
    - What is the optimal control strategy for driving a smart pneumatic stepper motor among Feedforward control, Error Correction strategy, and Adaptive Frequency strategy?
    - How does a smart stepper motor compare to a standard stepper motor?
2. What are the advantages and disadvantages of adding an Oscillator in the control system of a Pneumatic stepper motor?
    - Which is better: an oscillator or traditional valves using long pneumatic tubes?

1.2 Organization of the Thesis

The report of this thesis is organized in the following structure:

Chapter 2 provides background information on MRI, current MRI guided breast biopsy and robotic system developed to perform the biopsy, along with information on fiber optic sensors and information regarding the actuation principle used by the stepper motor and finally a state of the art Oscillator system which is a replacement of the traditional manifold system used in the previous robotic systems.

Chapter 3 discusses the different steps taken to design and integrate the optical encoder developed, the different control strategies developed using the optical encoder, and finally integration of smart pneumatic stepper motor with the oscillator system. The final section of this chapter describes the experiments done and the motivation behind them.

Chapter 4 shows the result obtained by performing the experiments and discusses what is the interpretation of the found result.

Chapter 5 draws the conclusion of the work done throughout the thesis where the main research questions and sub-question formulated in this chapter are addressed and answered. Finally ending this chapter with future recommendations where the further work that can be done to improve the smart pneumatics stepper motor and the oscillator system.

Chapter 2

Background

The purpose of this chapter is to provide information on the different aspects required to understand the purpose of creating a smart control for the MR safe Pneumatic stepper motor.

2.1 MRI

Magnetic Resonance Imaging (MRI) is a medical imaging technique used in radiology to form pictures of the anatomy and the physiological processes of the body. It uses strong magnetic fields, magnetic field gradients, and radio waves to generate images of the organs in the body. Since it does not involve X-rays or use ionizing radiations, which distinguishes it from CT and PET scans so it does not deal with hazards of ionizing radiation. Due to this reason, an MRI is seen as a better choice than a CT scan.

(a) MRI scanner

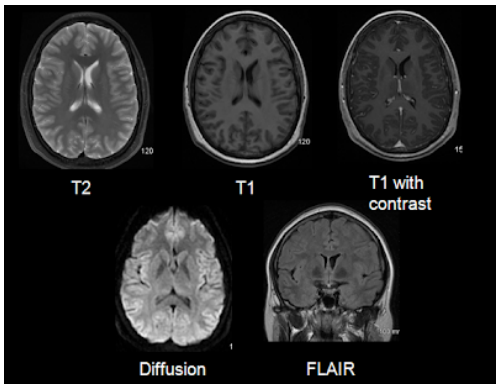

(b) MR Composite

Figure 2.1: MRI machine and Different results obtained by varying the parameter

MRI scanners use a strong magnetic field with oscillating gradients which resonate with protons. In a uniform magnetic field, the spin axes of all protons line up with this magnetic field. These spins can be deflected to a different alignment by superimposing an oscillating magnetic field on top of the uniform field, this is done by rapidly oscillating a set of electromagnetic coils. After turning off these oscillations the proton naturally falls back to its natural position, aligning the spin with a uniform magnetic field again and hereby transmitting a radiofrequency (RF) wave. The time needed to transfer from the excited to the original state is called the T1 relaxation time which is dependent on the type of tissue. Position information can be encoded by applying gradients to the magnetic field to define two-dimensional slices and using phase & frequency encoding schemes to distinguish rows and columns within that slice.

Several acquisition sequences are possible by changing various parameters such as the repetition time

(TR), echo time (TE), and others. Example sequences are the T1-weighted spin-echo which uses short TR and TE, while T2-weighted spin-echo uses long TR and TE times as it is observed in organs or parts which contain more water content as in edema, tumor, infarction, inflammation, and infection.

When a lesion is found which is classified as BI-RADS 3 or higher then a biopsy is generally advised. Biopsies can be done under ultrasound, x-ray, or MRI guidance. If the biopsy is not visible by ultrasound then MRI-guided biopsy is the next preferred method as MRI has the highest sensitivity among the other techniques and is also the safest method.

2.2 MRI Guided Breast Biopsy

Lumps or abnormalities in the breasts are often signs of a cancerous lesion in the breast. They are often detected by physical examination, mammography, or other imaging techniques. It is not always possible to tell from these imaging tests whether a growth is benign or cancerous. A breast biopsy is performed to take a sample from a suspicious area in the breast and then examine them to determine a diagnosis. This is done by using an image-guided needle biopsy using MRI or Ultrasound depending on the resolution needed.

If an Ultrasound biopsy is infeasible due to the invisibility of the lesion, then an MRI-guided biopsy is done. The breast is immobilized by two vertical plates. As seen in the image, one of the plates contains a rectangular grid which is used to get a better reference point to take a sample from the detected area. The

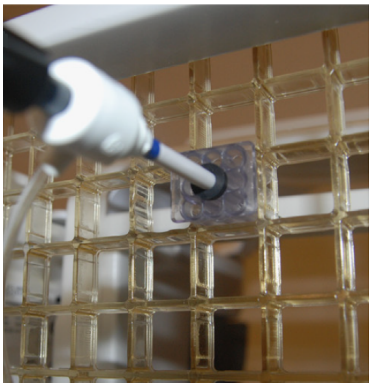

(a) Grid structure

(b) Biopsy method

patient is first scanned in MRI with and without the contrast agent and the suspicious lesion is localized and selected. Then using the biopsy software, the required grid and needle insertion depth is calculated. The patient is then moved out of the scanner and a stylet through a sheath is inserted to create access to the lesion. The stylet is replaced by an obturator and the patient is scanned again to confirm the location of the tip coincides with that of the lesion. If not then the last steps are repeated until the tip is at the right site. The patient is then moved again out of the scanner and the biopsy needle is inserted, usually taking multiple samples under the vacuum assistance. A localization clip is inserted and a final confirmatory scan is taken. The whole MRI-guided biopsy procedure takes around 45 to 60 minutes. A relatively thick needle is used to allow taking approximately ten samples and transport these through the needle to a container under vacuum assistance.

2.2.1 Current Benchmarks and Limitation

As discussed above the manual MRI-guided biopsy procedure requires the patient to move in and out of the scanner multiple times. The lesion is localized after a scan inside the scanner, but the needle can only be inserted outside the scanner by the radiologist. Although the breast is squeezed in-between two

plates, the lesion may still move due to breathing, involuntary muscle movement, and/or needle-tissue interaction. The aforementioned inaccuracies more or less force the radiologist to take away a relatively large volume of tissue samples. The vacuum-assisted biopsy device is an effective tool for this, but the thick needle results in significant tissue damage. The length of the MRI-guided biopsy procedure which is around 45-60 minutes combined with relatively high tissue damage makes the manual MRI-guided biopsy procedure inaccurate and inefficient.

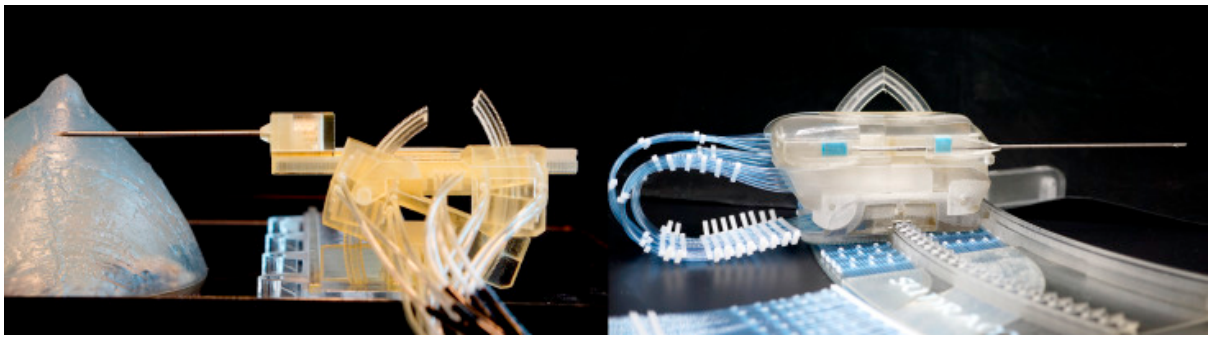

Figure 2.3: Stormram-4 (left)[5] and SUNRAM-5(right)[6]

The more efficient way is to use an MR safe robotic system which can improve the accuracy and efficiency of biopsies of MRI visible lesions in the breast. The found lesion's coordinate can be then transformed to the robot's coordinate system and using a robotic system will ensure accuracy and repeatability. Some examples of these robotic systems are: Stormram and SUNRAM series developed by the RAM department of University of Twente, MrBot by Stoianovici et al and Soteria RCM by Bomers et al.

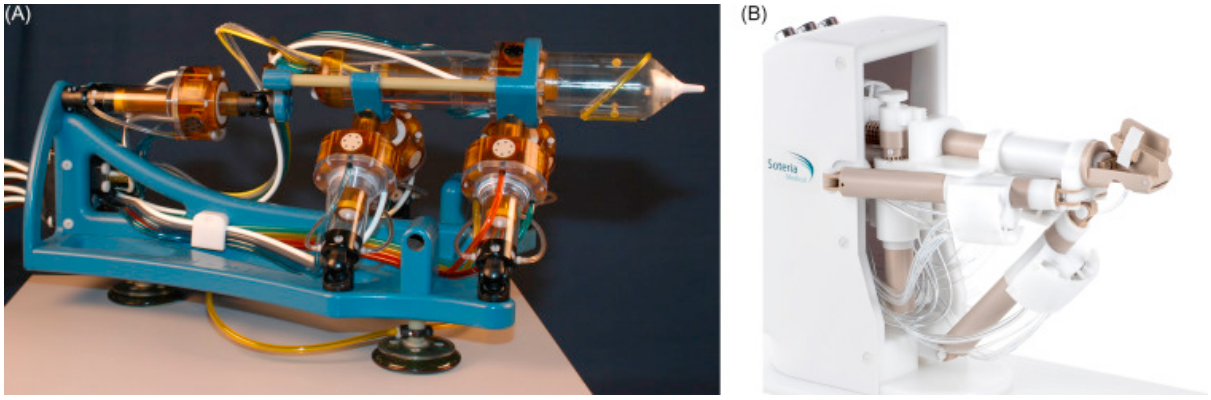

Figure 2.4: MrBot by Stoianovici et al.(left) Source: [7] and Soteria Remote Controlled Manipulator (RCM) by Bomers et al(right) Source:[8]

The latest Robotics system developed in the University of Twente, SUNRAM-5 an MR safe robotic system is used for MRI-guided breast biopsy. As per [5] and [6] the control strategy of stormram & SUNRAM series and design of the stepper motor [1], when one motor is commanded to move to a new position its valves are operated for the required number of steps at a given stepping frequency. As there is no position sensor, it solely works on feed-forward control strategy which limits its operating frequency and losses confidence in accuracy. Also, some of the other limiting factor for its lower step frequency is the length and diameter of the pneumatic tubes, the cylinder stroke volume and the valve's airflow. Currently the SUNRAM series (the latest) takes about 3 minutes and 25 seconds in average to complete the procedure [9]. In this whole procedure, the movement of robot is done for only around 1 minute and 38 second in average. This duration of time can further be reduced if the system had a feedback system in

order to account for the mistakes it might make and to increase the confidence of the procedure.

2.3 MRI compatible Sensor

In the last few years, there has been an increase in MRI-guided minimally invasive surgery. MRI is characterized by excellent soft-tissue contrast, high spatial resolution, the use of non-ionizing radiation, and image-based tracking and guidance. Thus there is a natural clinical aspiration to use live MR to monitor, feedback, guide, and control interventions. which brings the need for robotic systems which can perform the said procedure in an MRI environment faster and with higher accuracy. For performing the procedure faster and more accurately, the actuators of the robotic system or the robot itself should have a feedback system, this will theoretically increase the accuracy and safety of the system.

One of the conditions for using a feedback device inside the MRI scanner is that it should be safe to use in the given environment. The ASTM F2503 standard defines three categories of MRI devices which are: MR safe, MR conditional, and MR unsafe. The MR safe requirement implies that the device should be free from all the items which can interact with the magnetic field i.e. the device should be free of metallic, ferromagnetic, and conductive materials. Essentially, it should be free of any material which can cause distortion or create an artefact in the image produced by the MRI scanner. This will allow the device to work in all MRI scanners. MR conditional classification indicates that the device would work safely only for certain given conditions and the MR unsafe classification pose an unacceptable risk and should not be kept inside the MRI room.

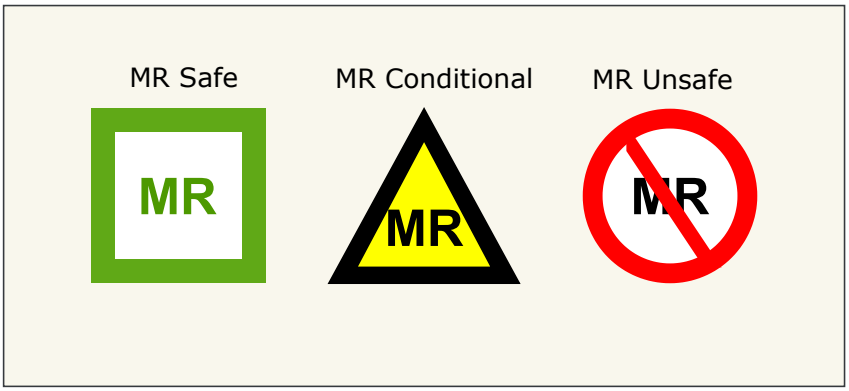

Figure 2.5: MR categories

From the energetic perspective, electricity excludes an MR-safe option, because electrical current inevitably generates electromagnetic waves causing imaging artefacts due to radiofrequency (RF) interference. Based on the definition of ”MR safe”, optical sensors are essentially the only type of sensors that can be used in an MRI environment safely.

2.4 Fiber Optics Sensors

The first application of optical fibres to the medical field enabled the illumination of internal organs during endoscopic procedures. These sensors are commonly grouped into two categories, Intrinsic and extrinsic sensors. In intrinsic sensors, the optical fibre is itself the sensing element and in extrinsic sensors, it is used as a medium for conveying the light whose characteristics are modulated by the measurand. The second type allows deploying the basic components of the Fiber optic sensor, i.e. the light source and photo-detector away from the sensing element, in order to develop a small size sensor and hybrid solution like MRI safe optical encoder.

According to the optical modulation mechanisms, fibre optic sensors can be classified as:

- Intensity modulation
- Wavelength modulation
- Phase modulation

Different working principles based on light intensity modulation allow developing Fiber Optic Sensors(FOS) for MRI application. In this kind of sensor, the measurand modulates the intensity of light passing through the fibre.

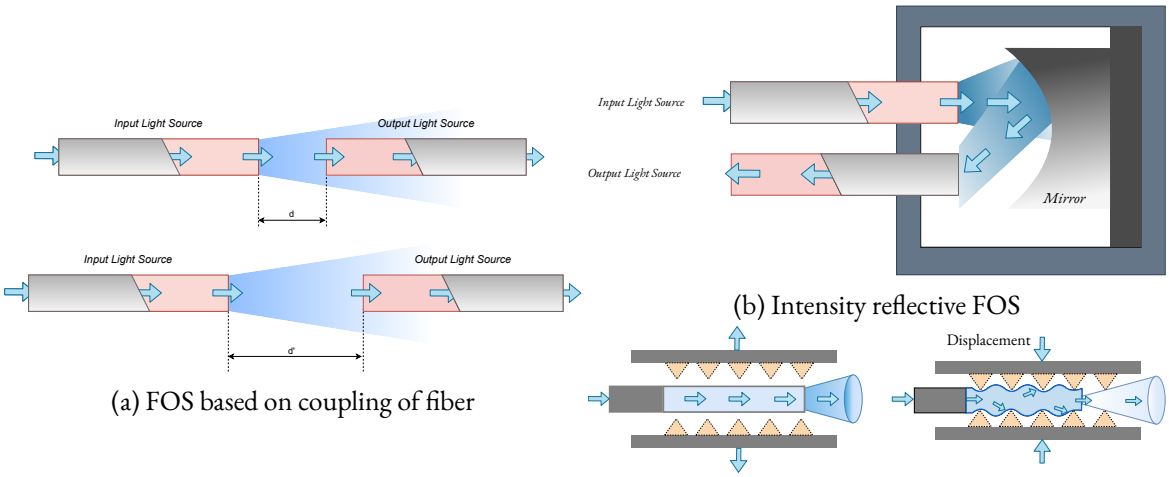

(a) FOS based on coupling of fiber

(b) Intensity reflective FOS

(c) Macrobending FOS

Figure 2.6: Different working principles of fiber optics using Intensity modulation mechanism

The working principle can be categorised in three different categories:

- FOS based on coupling between two or more fibres (cf. fig. 2.6a). In this type of sensor, the intensity changes as the distance between the two fibre changes. This type of sensor can also be modified to become an optical encoder by keeping the distance between the two fibre constant, and a succession of an opaque and clear section can send an analogue signal of on and off which can be then digitally converted using a photo-diode or photo-interrupter.
- Intensity reflective FOS (cf. fig. 2.6b), where a reflector is placed at a known distance at the end of one of the extremities of two optical fiber. The light transported by the first fiber is reflected back by the mirror to the second fiber which is coupled to a photo-detector. The intensity measured by the photo-detector is then used to measure the distance. The intensity readings are generally Voltage or current produced by the photo-detector.
- Macrobending FOS (cf. fig. 2.6c): their working principle us based on the light modulation owing to fibre bending. When a light ray enters the fibre, the amount of radiation lost into the cladding region increases as there are more bends in the fibre wire. This approach or property can be employed to measure physical parameters which can cause the bending such as force or torque.

There are multiple MR-safe force sensors present in the literature [10] but there is no MR-safe position sensor, although there are MR-compatible position sensors available [11] but, using these sensors creates artefacts in the MRI image which is not favourable.

2.4.1 Optical encoder and Quadrature signal

An optical encoder is a position sensor that is commonly used for measuring rotational motion or linear position of an actuator or a load. It consists of a shaft connected to a circular disc or a linear shaft, containing one or more tracks of alternating transparent and opaque areas. A light source and an optical sensor(photo-interrupter) are mounted on opposite sides of each track. As the shaft rotates, the light sensor emits a series of pulses as the light source is interrupted by the pattern on the disc. This output signal is then converted to a digital output by using a comparative circuit with the photo-interrupter.

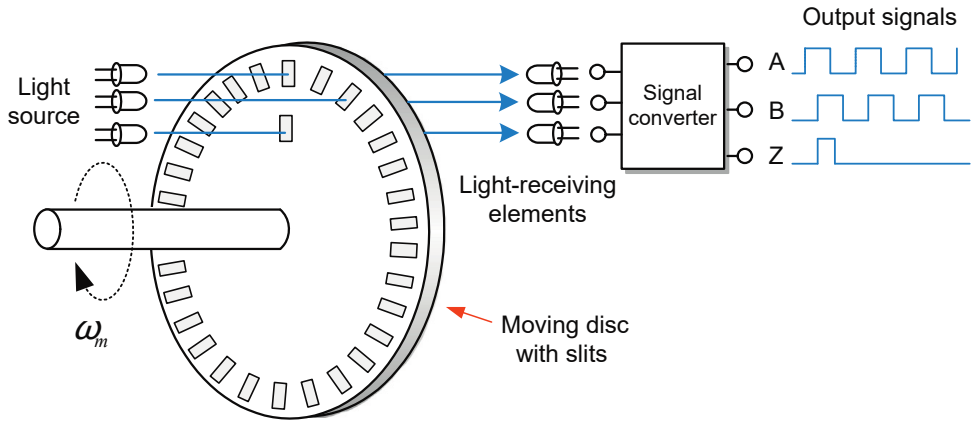

Figure 2.7: Rotation optical encoder Source: [12]

There are two types of optical encoder, incremental and absolute. An absolute optical encoder has several tracks, with different patterns on each, to produce a binary code output that is unique for each encoded position. In the incremental optical encoder, there are two tracks that are out of phase with each other, producing two outputs. The relative phase difference between the two channels indicates the direction of the encoder.

A rising edge on channel B after a rising edge on channel A means the encoder is moving in one direction, and a rising edge on channel B after a falling edge of channel A indicates the encoder is now moving in the opposite direction. A rising edge on channel B followed by a falling edge in channel B with no change in channel A indicates that the encoder has undergone no net motion. The out-of-phase A and B pulse train is known as quadrature signal which gives the direction of the encoder. Some encoders have a third channel which is used to give the index position.

2.5 Pneumatic Controller and Actuation Principle

An individual stepper motor is controlled by a pneumatic valve manifold which is controlled using an Arduino and can be connected to a user interface as done in [5]. The fig. 2.8b shows a schematic of the controller including one pair of valves for controlling one stepper motor. The stepper motor is independently operated by a pair of 5/2-way valves of type Festo MHA2-MS1H-5/2-2 (Festo AG & Co. KG, Esslingen, Germany) connected to a 5 m pneumatic tube. This allows the MR unsafe controller to be placed outside the Faraday cage of the MRI to eliminate the possibility if RF interference and safety issues.

The pneumatic connection scheme and operating sequence are shown in fig. 2.8b. As stated by V. Groenhuis and S. Stramigioli in [1], the five states are numbered 0-4 (c.f. fig. 2.9), shows the consecutive position of the piston and rack when it is operated from left to right. Exactly one piston can be fully engaged on the rack. This is always the piston that moved formerly and independent of the direction of load. The piston that moved most recently acts as a wedge between the rack and the cylinder housing, effectively eliminating any backlash in the motor by design.

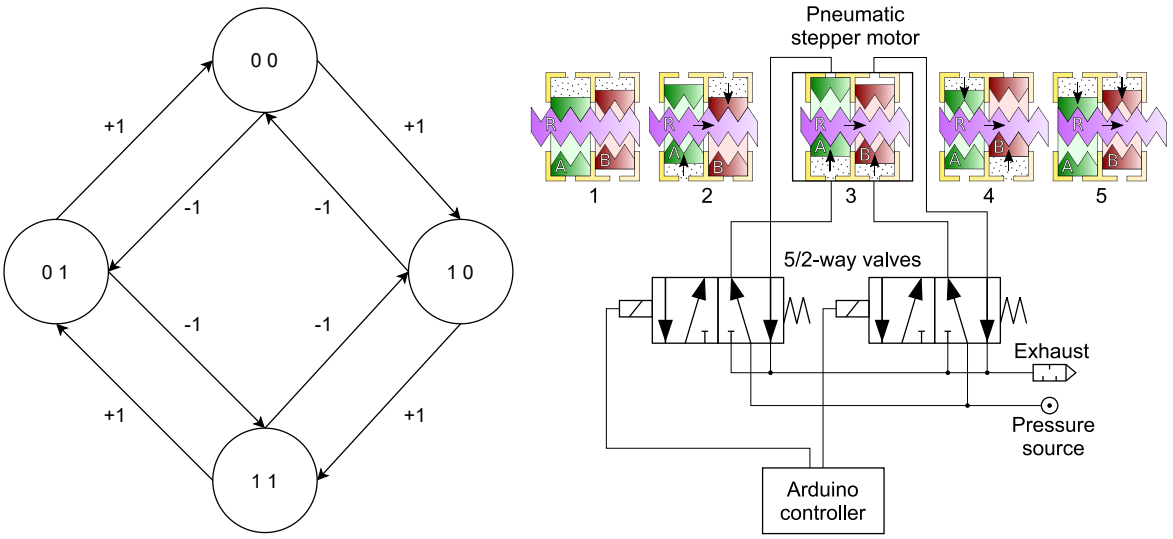

(a) State machine node for quadrature signal A/B channel (b) Pneumatic control schematic and five consecutive states of a single stepper motor Source: [5]

Figure 2.8: Control scheme for Pneumatic stepper motor

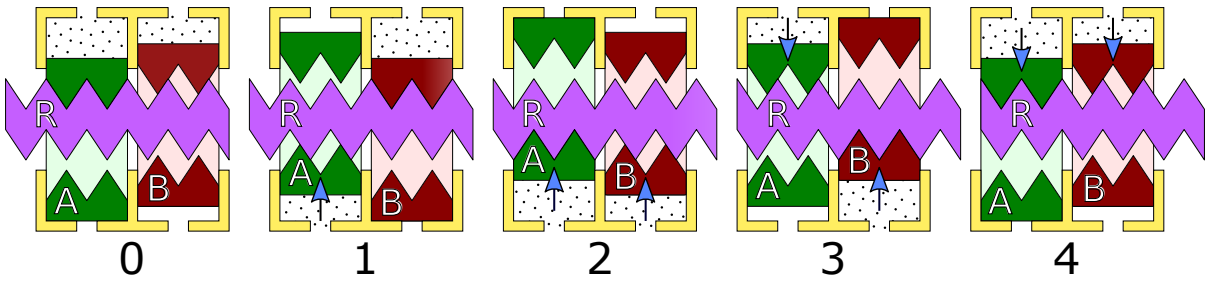

Figure 2.9: Five consecutive states of a single-speed linear stepper motor with the housing (yellow), rack (purple) and pistons (red and green) Source:[1]

The control sequence can also be explained by fig. 2.8a, the nodes are the state of the individual valves. Changing the bit in a particular direction changes the direction of the stepper motor. The bit written in the figure is the state of the two valves. Following the pattern, the motor can be driven in a forward or backward direction.

2.6 Pneumatic Oscillator

The Pneumatic Oscillator works on the principle of a Ring oscillator circuit. A ring oscillator circuit is composed of odd numbers of NOT gates in a ring, whose output oscillates between two voltage levels, representing true and false. The NOT gates or inverters are attached in a chain and the output of the last inverter is fed back into the first (cf. fig. 2.10a).

The Pneumatic oscillator is based on the same principle of a ring oscillator but, here the circuit is made of one inverter and one follower which can be seen in fig. 2.10b. To make this circuit into a mechanical-pneumatic circuit, the gates are changed into a 12/2-way pneumatically actuated valve. As the name suggests the valve has 12 ports and 2 states and in fig. 2.11, of the 12 ports, 4 of them are output ports and the other 8 are divided between the exhaust port and pressure port. A pneumatic valve has two states, Normally open (NO) and Normally close (NC). The two states can be seen from the left and right side of the valve, upon switching the state, the pressure and exhaust ports that are connected to the output ports are switched.

(a) Principle of a simple 3-inverter ring Oscillator

(b) Principle for pneumatic oscillator system

Figure 2.10: Electrical circuit for ring oscillator and oscillator system principle

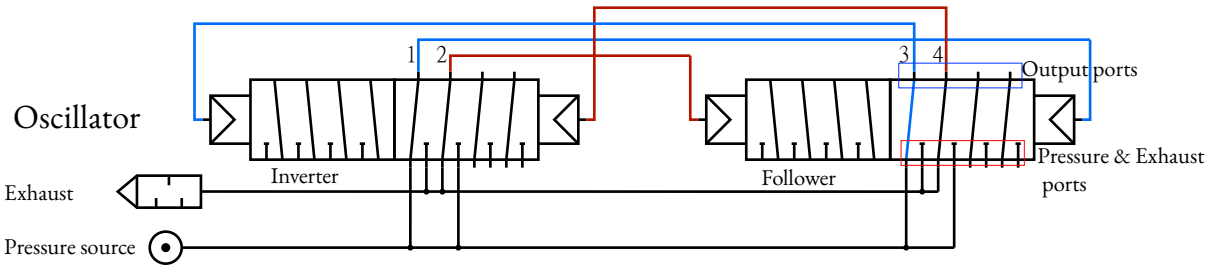

Figure 2.11: Pneumatic-mechanical representation of a simple oscillator circuit comprising of an inverter and follower valve Source: [2]

In order to make a simple pneumatic oscillator circuit, two 12/2 way valves are interconnected in which the left valve acts as an inverter and the right valves as a follower. Figure 2.11 shows the pneumatic representation of the oscillator circuit. The pneumatic lines represented by blue lines in the image are the ones through which pneumatic air is passing through and the red lines show that they will be actuated once the switch changes to the left side. Pneumatic line-1 is giving a signal to the follower valve, which switches the right side of the second 12/2 way valve. This enabled the pneumatic line-3 to get connected with the pressure source and further allowed the left side of the first valve to switch on. This way in the next iteration, pneumatic line 2 will be connected to the pressure source which would switch the left side of the follower valve to get the pressure source. This is how the inverter and follower trend is used to switch the states of this system and allowing oscillation between state 1 and 0 of the valve making a pneumatic quadrature signal as a result.

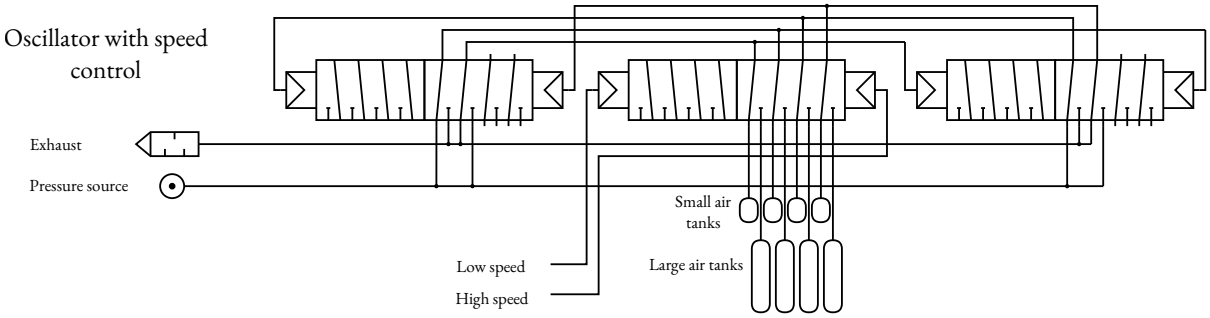

Figure 2.12: Oscillator speed mode pneumatic circuit Source: [2]

This system was converted to a mechanical system which was completely 3D printed to make it MR safe. The prototype uses screws that are metallic and can be easily replaced with nylon screw and bolt. The physical system is made of six 12/2-way pneumatically actuated valves of which two valves are responsible for switching the direction (fig. 2.13), one is responsible for changing speed mode (fig. 2.12) and two are used to create quadrature signal which is then connected to a pneumatic stepper motor to actuate it, the last valve is unused and can be used as a spare.

The speed mode of this system can be explained from fig. 2.12, the two different tanks are responsible for switching the speed. The tank dimension decides the time delay between switching the state of the

inverter and the follower valve. A single 12/2-way valve is used in order to switch between the two tanks i.e. switching between 'Low speed' and 'High speed' mode, the four output ports are connected with air tanks and the air tanks' dimension is changed depending on which side of the valve, i.e., left for low speed and right for high-speed mode is actuated.

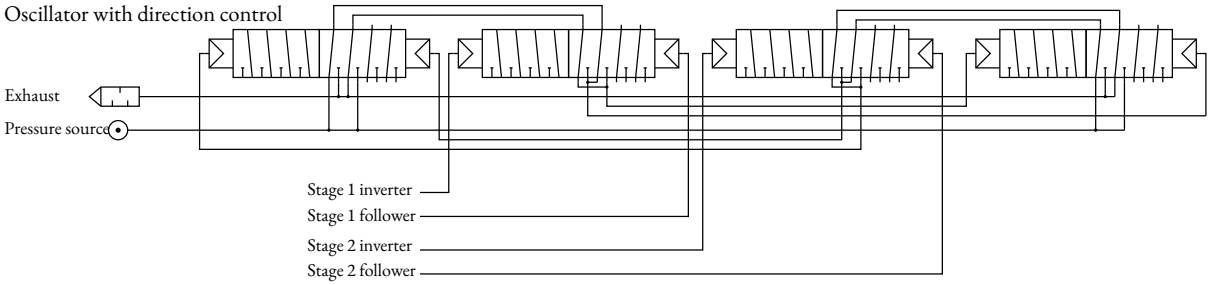

Figure 2.13: Oscillator Direction mode pneumatic circuit Source: [2]

The pneumatic circuit for direction control can be explained using fig. 2.13, the direction of the pneumatic quadrature signal generated as explained before is done by the follower and inverter valves, the order of inverter and follower valves decides the order of quadrature signal which is done by the two additional valves present in fig. 2.13. In case the direction of movement is set to forward or clockwise, the first 12/2-way valve shown in fig. 2.11 becomes a follower and the second valve becomes the inverter. The extra valves present in fig. 2.13, is responsible for switching the behaviour of the valves.

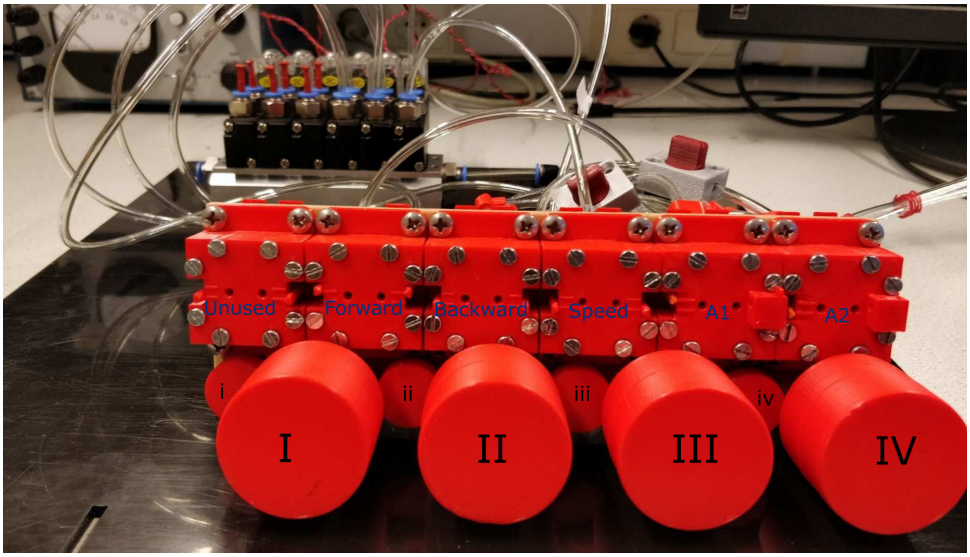

Figure 2.14: **Oscillator system:** It comprises of 6, 12/2-way pneumatically actuated valves

The complete system would include the speed mode attached which would decide the duration after which the state switches. The complete mechanical realization of the system can be seen from fig. 2.14. One extra valve is present here which is unused and serves as a replacement in case a valve stops working. The last two valves are responsible for generating the pneumatic quadrature signal and is connected with the pressure source directly and gets the signal from switching from the direction valve. The other valves are controlled with a 5/2-way solenoid valve which is controlled using an Arduino controller. This way the whole system is MR safe and still able to generate the required force and speed acting as an improved version of using the traditional approach to control the Pneumatic stepper motor. The only problem with this system is that it generates the quadrature signal for as long as the pneumatic signal is sending the signal and cannot account for the number of steps taken without any feedback system which makes controlling this system very complicated.

2.7 Approach

The different MR safe Robotic system developed for MRI guided breast biopsy have proven to be an improvement on the older method where the vacuum-assisted biopsy was performed by shortening the time duration. The major draw back of the existing MR safe robotic system was that there was no feedback system and auto-calibration which forced the robotic system to work at a lower speed increasing the overall time duration of the procedure.

The aim of this thesis is to create a new MR safe optical encoder which is then incorporated into the MR safe pneumatic stepper motors that are used in Stormram-4 [5] and SUNRAM-5[6] robots but specifically T-49 stepper motor. Further different control strategies using the feedback system was investigated and finally, the oscillator system which is an MR safe version of the controller manifold, a replacement of solenoids is integrated with the MR safe pneumatic stepper motor. The performance of each system was evaluated and compared.

Chapter 3

Materials and Methods

This chapter deals with the design choices made in order to make the MR safe Optical encoder and its integration in the Stepper motor and Oscillator. Later the MR safe optical encoder is used to develop different control strategy and smart features to efficiently run the stepper motor.

3.1 Design of MR Safe Optical Encoder

In order to create a position sensor for the feedback system in MR safe Pneumatic stepper motor, few conditions are needed to be fulfilled by the optical encoder to make it MR safe. The conditions are stated below:

- The sensor should not cause any RF interference to MRI scan, i.e., it should not have any electrical part inside the Faraday cage of the MRI
- The resolution of optical encoder should be at least as much as the step size of stepper motor, i.e., 1 mm.
- Designed encoder should not effect the performance of the stepper motor, i.e., it should not cause major changes in the design of the stepper motor.

These conditions were the only design choices that needed to be taken care of in order to make an MR safe optical encoder. Initially, a mock-up of the sensor housing fig. 3.1a inside the stepper motor was created to test the feasibility of the sensor. After taking some initial reading using a 5 m fiber-optic cable for sending light source and for receiving it to photo-interrupter.

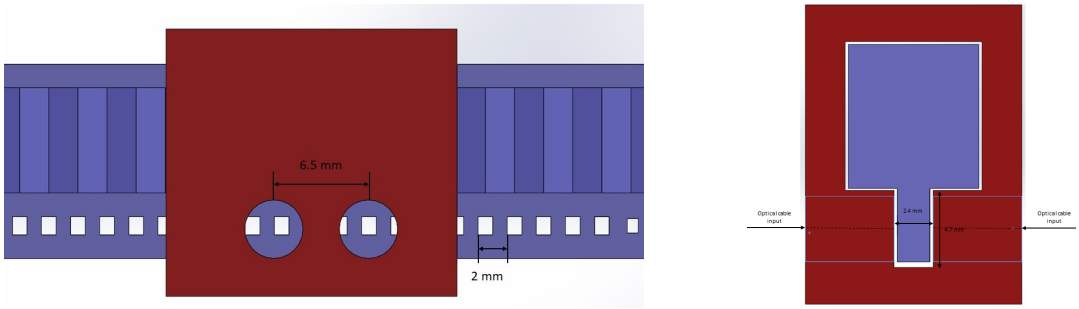

(a) Side view of Mock-up sensor housing (b) Front view of Mock-up sensor housing

Figure 3.1: Mockup sensor design

In order to get a quadrature signal from an encoder, the two signals should be out of phase by 90°. But this is only for a rotary encoder, for a linear encoder it should be out of phase by 25% of the step size or resolution of the track. The value 25 % is taken in order to generate 4 different phase during one step which generates the quadrature signal. The port for the optical fiber to connect in fig. 3.1a is separated by a factor of 0.25×step size×n, where 'n' is decided by the size of the optical fiber being used and the 3D printer resolution. In this project, the fiber being used is HFBR-RUS100Z Series[1](Plastic Optical Fiber) whose thickness is 2 mm. In order to make it easier for the 3D printer to print the ports correctly and for the ease of integrating the fiber in the housing we set the factor to be: n = 13 for the mock-up sensor and n = 7 when it was integrated with the pneumatic stepper motor. This made it easier to integrate fiber in the sensor housing without causing any stress in the fiber itself.

The design of the electrical circuit used for the sensing parts is very straightforward. The LEDs each have their current limited by 120 Ω resistor and the phototransistors were first connected in series with a variable resistor. The variable resistor is used to get the best sensitivity and once found, the resistance was used for the other phototransistors. One of the major issues with phototransistors is that they are prone to get noise from surrounding light. In order to solve that, a housing component for the LEDs and the photo-interrupters was designed along with the connectors for optical cables (fig. 3.2a), this way no noise from the surrounding was able to get inside.

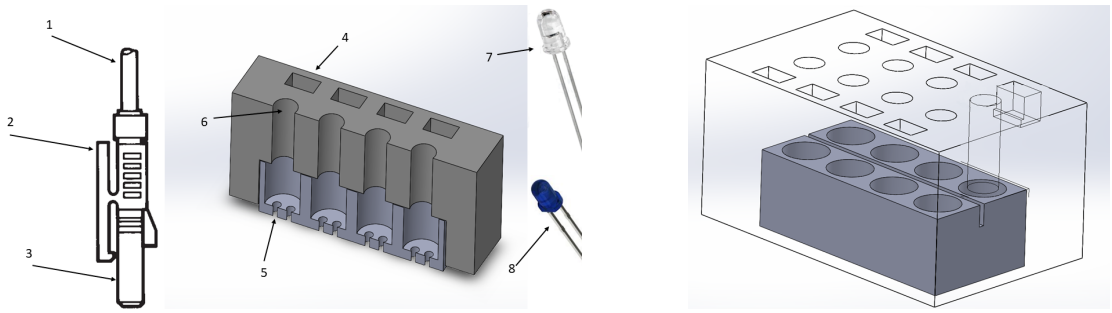

(a) Sensor housing components (b) Sensor housing cross-section view

Figure 3.2: **Sensor housing design.** In order: 1. Simplex latching cable output; 2. Latching mechanism; 3. optical cable input; 4. latching location; 5. space for cathode and anode of photo-interrupter and LED; 6. optical cable input location in sensor housing; 7. LED; 8. photo-interrupter

The sensor housing for the electrical component is divided into two parts which can be separated, it was done in order to make the assembly and 3D printing easier. The first row of the lower part contained all the LEDs and the second row contains all the photo-interrupters. The upper part is for the Optical fiber connection. As shown in fig. 3.2a, the grey part holds the connection for optical cables and the other part contains LEDs and Photo-interrupter.

3.1.1 Working Principle

In order to make the encoder work for MR safe condition, two different working principles were combined to make the encoder MR safe. The working principle of intensity modulation used by coupling of fibers and incremental optical encoder was used. The optical cables are used for the transmission of a light source to the sensor housing and another cable transmits it to the photo-interrupter. According to the principle of intensity modulation for the case of coupling of fibers fig. 3.3, as the separation between the two coupled fibers increases, the intensity reduces. While making the mock-up sensor housing, the distance between the two fibers was set to the same value as it would have been in the stepper motor to check the feasibility of this method. Reading were taken for the two cases, i.e. when the light was passing through the slit and when no light was passing, the analogue output is shown in fig. 3.4a.

[1] https://docs.broadcom.com/doc/AV02-1508EN

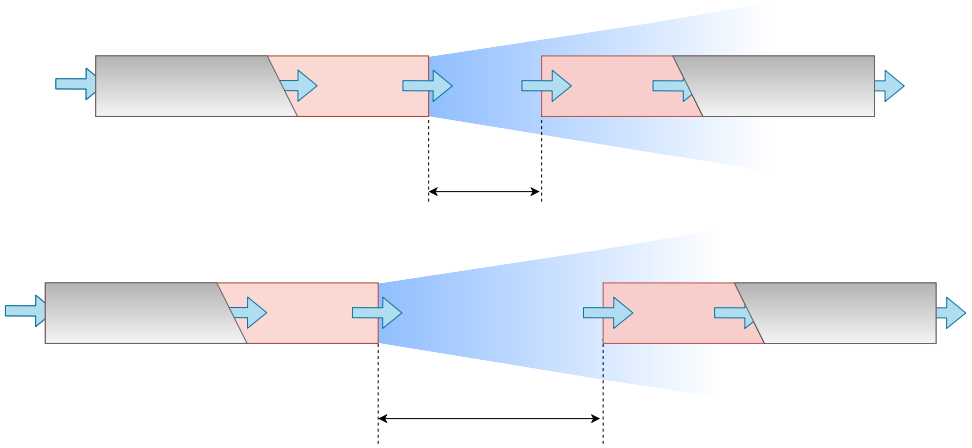

Figure 3.3: Intensity modulation using coupling of fibers

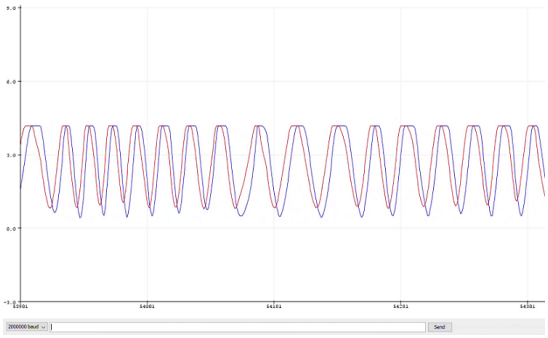

(a) Analogue output of the mock-up sensor

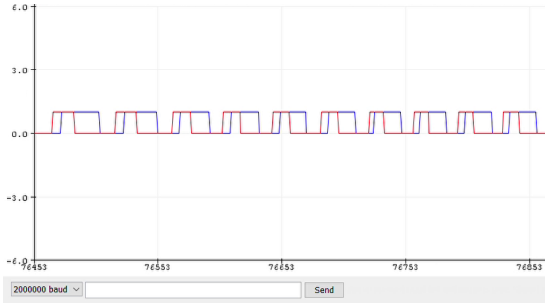

(b) Digital output after testing with the mock-up sensor housing

Figure 3.4: Analogue and Digital quadrature output from Mock-up sensor

It is clear that the sensor unit 5 m away from the sensor housing is able to keep track of the change even though the light source has to travel 5 m from led to the sensor house and then from the sensor house to the photo-interrupter, travelling a total distance of 10m. The difference between the two cases was 4.3 V for when no light is passing through or the 'OFF' case and 1.1 V when light is passing through or the 'ON' case. The difference between the two cases was enough to use a simple comparator to change them in digital signal as seen in fig. 3.4b. The response time is fast enough to work with the stepper motor. The step resolution for the encoder is 1 mm and since using the 5 m optical cable allows the sensing unit to be outside the MRI room, the optical encoder fulfilled all the condition required for making it MR safe. After getting satisfactory readings from the circuit (shown in fig. 3.4b), the optical encoder's sensor housing is then integrated with the Pneumatic stepper motor T-49.

3.1.2 Integration with Pneumatic Stepper Motor

In order to integrate with the Pneumatic stepper motor, few changes were also needed to be made in the design of the stepper motor itself. To incorporate the housing, changes which were made did not alter the performance of the stepper motor but were additional compartment and change in dimension of few parameters of the rack. Due to the change in rack, few changes were needed to be made in the middle part of the stepper motor in order to accommodate this change in the stepper motor. These changes can be seen from fig. 3.5a, the final design of the stepper motor can be seen from fig. 3.5b

Due to the presence of the optical encoder, a new control schematic was also designed in order to combine the sensor housing with the controller so as to take direct advantage of the feedback system to create different control strategies. Using the schematics shown in fig. 3.6, two different control strategies were

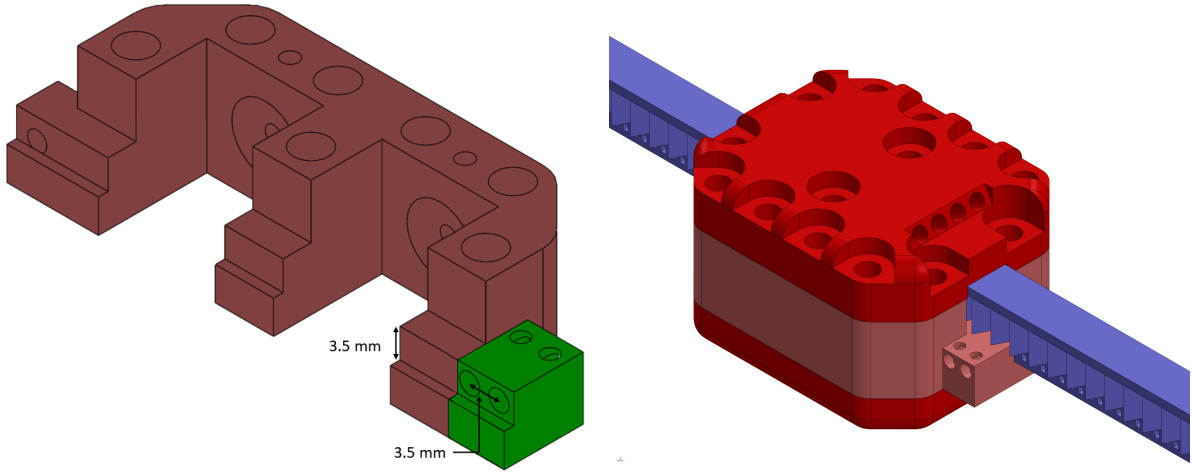

(a) Middle part of T-49 Pneumatic Stepper motor with optical cable housing (b) T-49 Pneumatic stepper motor with optical encoder

Figure 3.5: Comparison of middle part of T-49 stepper motor before and after sensor integration

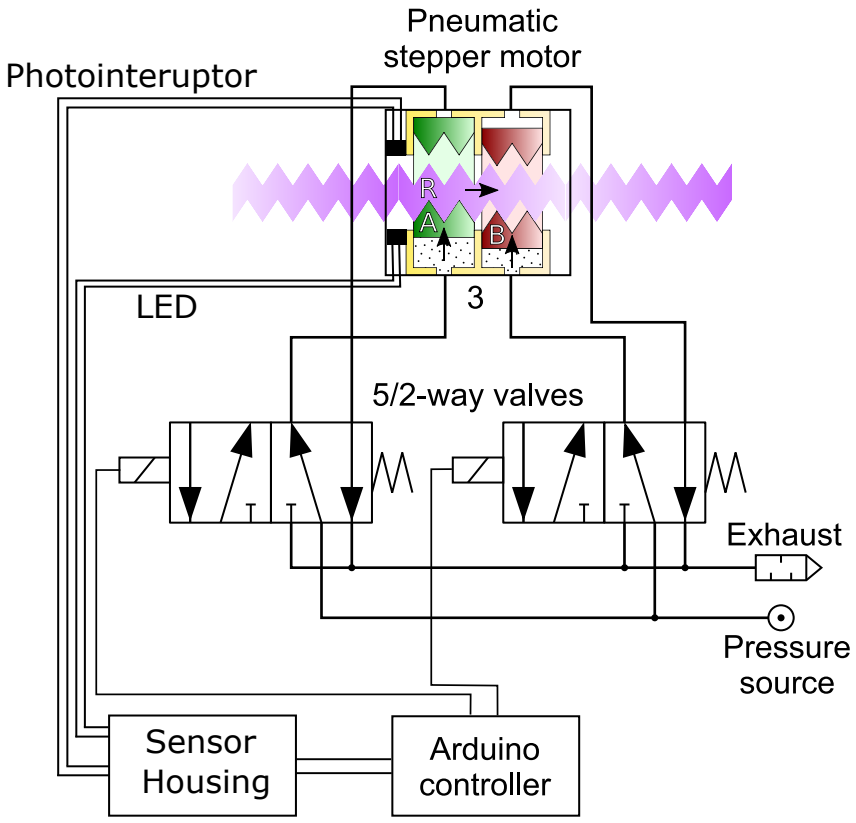

Figure 3.6: Schematic for Pneumatic stepper motor integrated with optical encoder

developed which are: i) Error Correction Strategy and ii) Adaptive Frequency Strategy.

3.2 Error Correction Strategy

The first control law was developed in order to deal with the known problem of Pneumatic stepper motor, while working at high step frequency it starts missing a few steps due to slipping caused by insufficient pressurization of chambers. To deal with this a simple error correction strategy was developed. In this control strategy, the controller kept track of the step taken by comparing the programmed step to the actual step taken which is tracked by the optical encoder. The algorithm being used by this control strategy is discussed in the next sub-section.

3.2.1 Methodology

The control strategy follows the algorithm represented by the flow chart shown in fig. 3.7.

The linear actuator on which the optical encoder was integrated is the T-49 MR-safe stepper motor. This particular stepper motor has a resolution of 1 mm. The number of steps required to complete the input distance is just the conversion of input distance in millimetre or simply take the input distance in millimetre.

In the algorithm, the controller keeps checking the step taken at the end of each step duration, the step duration is decided by the step frequency which is a fixed input parameter for the controller. At the end of the step duration, the controller switches states of the solenoid which in turn sends the pneumatic signal to the stepper motor by pressurizing the respective chamber to move the piston which in turn pushes the rack and the stepper motor moves, the change in the state responsible for moving the stepper motor can also be seen from fig. 2.9. If at the end of step duration, the optical encoder does not detect any step, the stepper motor has slipped and correction is made on the commanded step by reducing the step-taken. This process is repeated unless the recorded step-taken or feedback step is equal to input distance.

3.3 Adaptive Frequency Strategy

The control strategy developed follows the algorithm represented by the flow chart shown in fig. 3.8.

Pneumatic actuators exhibit highly non-linear behaviour given by factors like air compressibility, friction in pneumatic tubes, mass flow/ volume flow rate characteristics [13]. In order to get a precise motion control or force output according to the different conditions, proper mathematical models and experimental identification procedures are required. This highly complicates designing the control law for the pneumatic actuators and it is even more complicated for an MR safe pneumatic actuator, due to which a pneumatic stepper motor is generally used for actuation purpose. Without a feedback system, the best way to drive a pneumatic stepper motor without a feedback system is by the feedforward method. But after integrating the pneumatic stepper motor with an optical encoder, we can efficiently control the stepper motor by observing its behaviour using the distance travelled vs time plot obtained using the optical encoder and error correction algorithm. This lead to a new control strategy which is described in the section 3.3.2. But before the control strategy can be explained, the approach taken or the limiting function created for this strategy has to be explained which is done in section 3.3.1.

3.3.1 Approach

After observing the performance of the stepper motor using the Error correction strategy, a detailed study of the stepper motor behaviour was done. Upon looking at the pressure step response shown in fig. 3.9

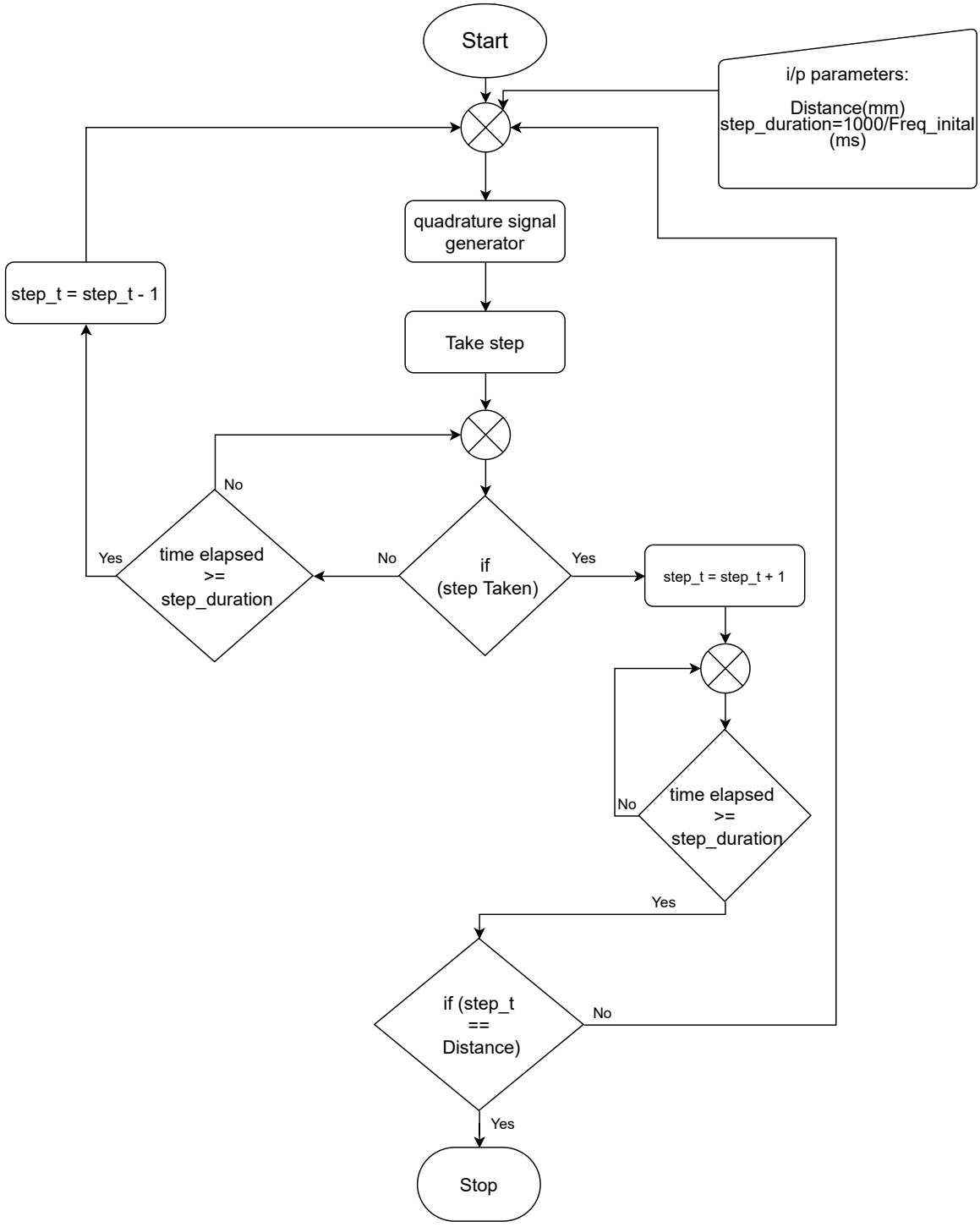

Figure 3.7: Error correction strategy algorithm

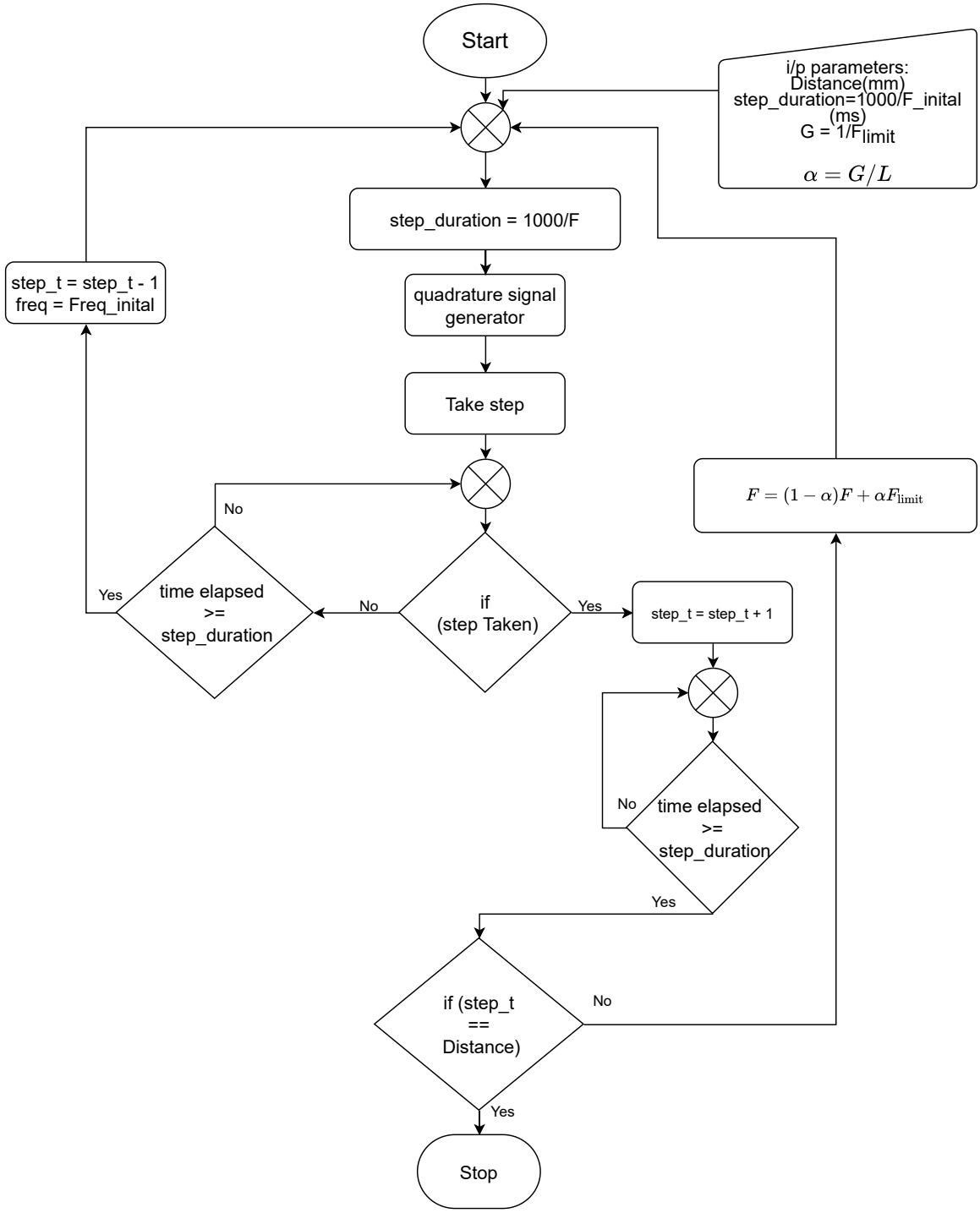

Figure 3.8: Adaptive frequency strategy algorithm

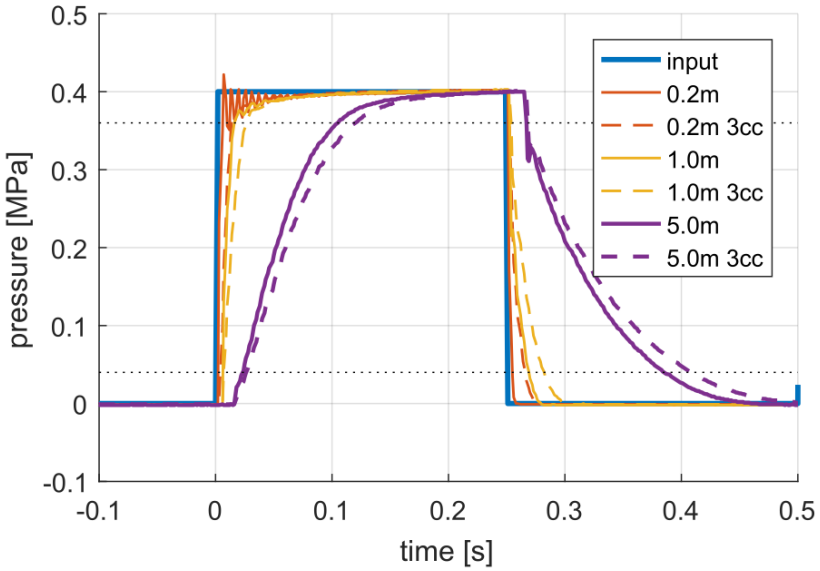

Figure 3.9: Pressure response for three different tube lengths, with and without 3cc reservoir Source: [1]

taken from the result section of Rapid Prototyping High-Performance MR Safe Pneumatic Stepper Motors [1], the pressure response for 5 m pneumatic tube length showed the same behaviour as a charging-discharging of a capacitor from an RC circuit. The discharging curve observed in the figure shows that it takes around 0.25 seconds to completely discharge the air. Using this property shown by the 5 m pneumatic tube, the adaptive frequency strategy was developed. In this strategy, the time delay of discharging is taken advantage of by gradually increasing the step frequency. This way, the stepper motor's chamber maintains the momentum of its motion and is able to work at a higher step frequency.

Using this as an inspiration, the limiting function was designed by exponentially increasing the step frequency. The limiting function followed an exponential equation which is described below:

$$\alpha = \frac{G}{L} \qquad G = \frac{1}{f_{\text{limit}}} \tag{3.1}$$

$$f_i = (1 - \alpha) f_{i-1} + \alpha f_{\text{limit}} \tag{3.2}$$

Changing the parameter of eq. (3.2), the controller can control the rate and the limiting value till which the frequency would increase. The effect of changing the parameter can be seen from fig. 3.10. The effect of changing parameter L can be seen from fig. 3.10a, in this figure, the G parameter was set to 0.04 due to which the limiting frequency became 25 Hz. In fig. 3.10b, the effect of changing the G parameter can be seen, in this figure parameter L, the rate at which the step frequency would increase is kept constant and G is being varied, due to which the controller limits to a different frequency.

3.3.2 Methodology

The control strategy follows the algorithm shown in fig. 3.8. In this strategy, the controller keeps increasing the step frequency exponentially as explained in section 3.3.1. The controller keeps increasing its step frequency using the limiting function until it makes a mistake. After making a mistake, the controller sets the step frequency to the initial frequency at which the stepper motor started moving.

The step frequency at which the stepper motor makes a mistake is recorded and is used to set as the limiting frequency for the next run. This way, the stepper motor can be calibrated once, and then this calibration

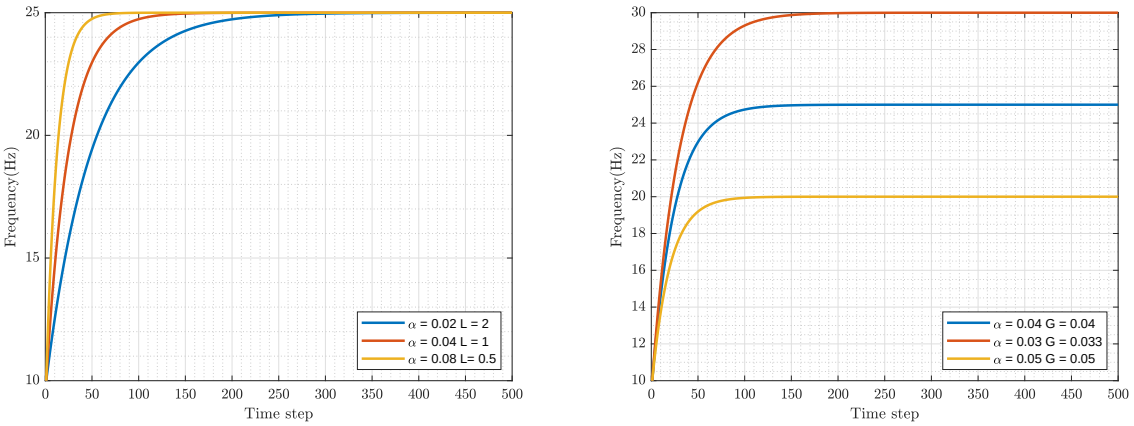

(a) Effect of varying L parameter in α

(b) Effect of varying G parameter in α

Figure 3.10: **Effect of changing α on the rate of change of frequency**: increasing α increases the rate at which frequency increases

can be used for the entire session the stepper motor is used. The next calibration would be done when the stepper motor again makes a mistake even though it was calibrated before. The other parameters are similar to that of the error correction strategy [fig. 3.7], i.e. the controller still accounts for the missing steps.

3.3.3 Analysis

In this section, the effect of different gain value of the adaptive frequency strategy is shown. In fig. 3.11, the effect of different gain value can be seen. How changing the gain value and initial step frequency (as stated in the legend of the figure) changes the performance of the stepper motor.

In the adaptive control method, the stepping frequency is increased exponentially to a limiting value until the stepper motor slips and misses a step. The stepping frequency is then set to its initial value, and then it rises again. The rate at which it is increased also affects the performance of the stepper motor. Fig.3.11shows the different gain value and the results obtained are after tuning the gain value which would result in cases which makes the least error.

To find the gain value for this session, first, the stepper motor is calibrated by initially giving a very low gain value, which results in a very high saturation for the step frequency. The controller then records the frequency at which the stepper motor made the first error and uses it to set the new gain value, which is used to run the stepper motor, and the result is shown in fig. 3.11. fig. 3.11.

From the figure you can see that the stepper motor is faster after calibration, the red line which allowed the step frequency to go from 6 Hz to 24 Hz encountered an error when step frequency became 21 Hz by updating the frequency using the limiting fuction, this gave an upper limit to the step frequency at 21 Hz. Various other tests were also done in which the initial freq was changed in order to get the fastest response for covering 100 mm. The blue line shows the fastest response, covering 100 mm in 5 seconds. This gain value and initial frequency gave the fastest response and it can be considered to be the new calibrated value for the stepper motor in this run.

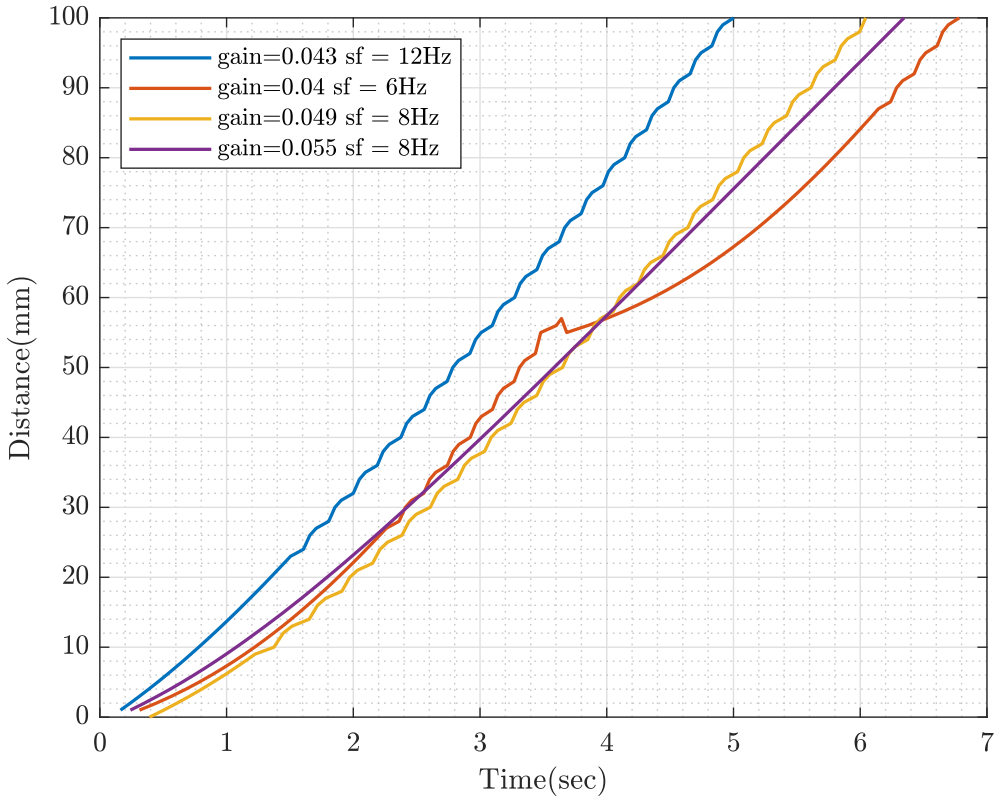

Figure 3.11: Tuning gain value for Adaptive Frequency control strategy

3.4 Pneumatic Oscillator System

The Oscillator system is an MR safe replacement for the valve manifold, it generates a pneumatic quadrature signal in two directions depending on the direction of motion required. It has 3 switches as can be seen in fig. 3.12, two of them are used to set the direction of the quadrature signal and as a result, set the direction of the stepper motor. The last switch is a speed mode, moving the stepper motor in two-speed mode.

The pneumatic oscillator generates a quadrature signal for the duration of time it is activated but there is no way to be sure the number of times the states have been changed, i.e. the number of steps the quadrature signal has generated. In order to use this system with the pneumatic stepper motor, a feedback system is required.

3.4.1 Integration

Controlling a Pneumatic stepper motor without any feedback from an oscillator would be very complicated as for this to happen we would need to work on the dynamics of the pneumatic stepper motor and the behaviour of the oscillator, which is very complicated to determine. Thus the presence of an optical encoder in the stepper motor, made it easier to make a controller for this combination of system. In order to control the pneumatic oscillator from outside of the Faraday cage, the three switches are connected with three 5/2-Solenoid valves in order to send signals for controlling the direction and the speed of the stepper motor. The oscillator is getting the source pressure directly, which subsequently reduced the distance between the source pressure and stepper motor from 5 m to 1 m or less. This increased the overall force output of the stepper motor which also made the slipping of the step even less which overall increased

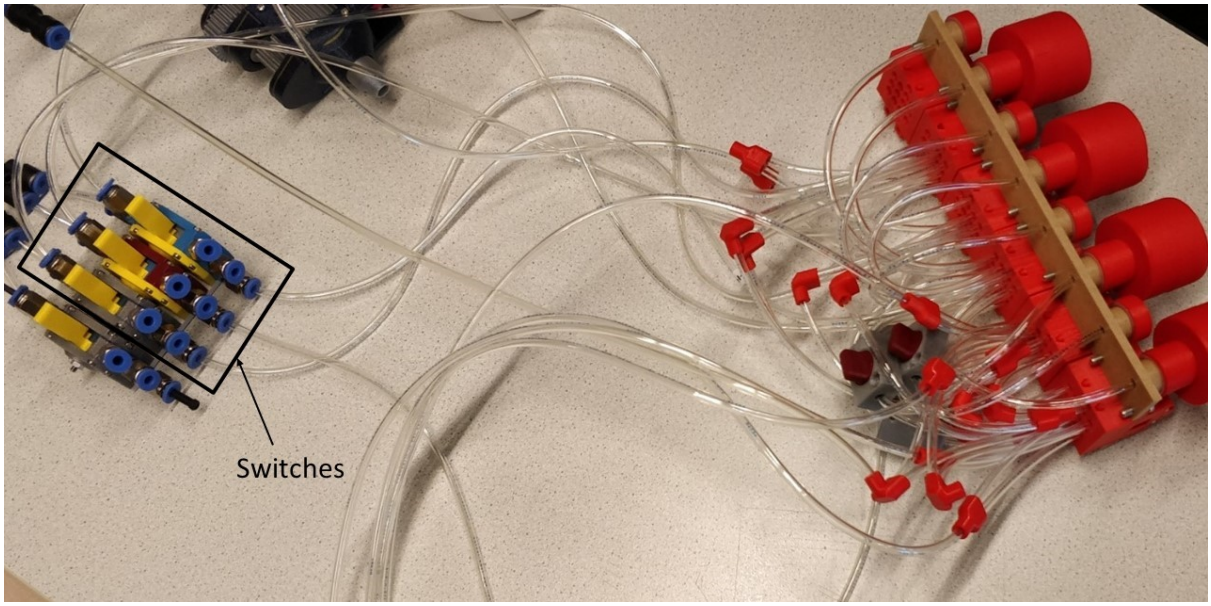

Figure 3.12: Pneumatic Oscillator

the average velocity of the system. The only problem with controlling the MR safe pneumatic stepper motor by integrating an oscillator was that there was no accurate way to know the number of steps taken by the stepper motor accurately, this was solved through the integration of the MR safe optical encoder with the pneumatic stepper motor. The control schematic which integrates all the component required to run this system is represented in fig. 3.13 and the real system can be seen in fig. 3.15.

3.4.2 Methodology

The control strategy for this system is fairly simple. The three solenoids which are now the switches control the Oscillator system and is 4 m away and the stepper motor is 1m away from the solenoid. This makes the total distance between the stepper motor and all the electrical component to be 5 m. The control schematic can be seen from fig. 3.13 and the control strategy can be seen from fig. 3.14.

Table 3.1: Chamber's state depending on sequence and direction

Sequence	Clockwise		Counter-Clockwise	
	Chamber-A	Chamber-B	Chamber-A	Chamber-B
I	0	0	0	0
II	1	0	0	1
III	1	1	1	1
IV	0	1	1	0

The controller gets the input position of the stepper motor using which the direction of the stepper motor is decided. The two directions switch for the oscillator as shown in fig. 3.13, decides if the stepper motor has to go in a forward or backward direction. If the stepper motor has to go in a forward direction or clockwise direction, the pressurized air goes into chambers represented by Roman numbers and follows the sequence of I→II→III→IV and if the stepper motor has to go in backward direction or counter-clockwise direction then the pressurized air goes into chambers following the sequence of IV→III→II→I or follow the sequence of counter-clockwise direction shown in table 3.1. Each sequence marks one step and the sequence represents the state of the chambers of the stepper motor which can be seen from table 3.1. The state '0' represents that the chamber is not getting any pressurized air and state '1' represents that it is. The speed mode switch decides if the chambers with capitalized Roman numbers are to get the

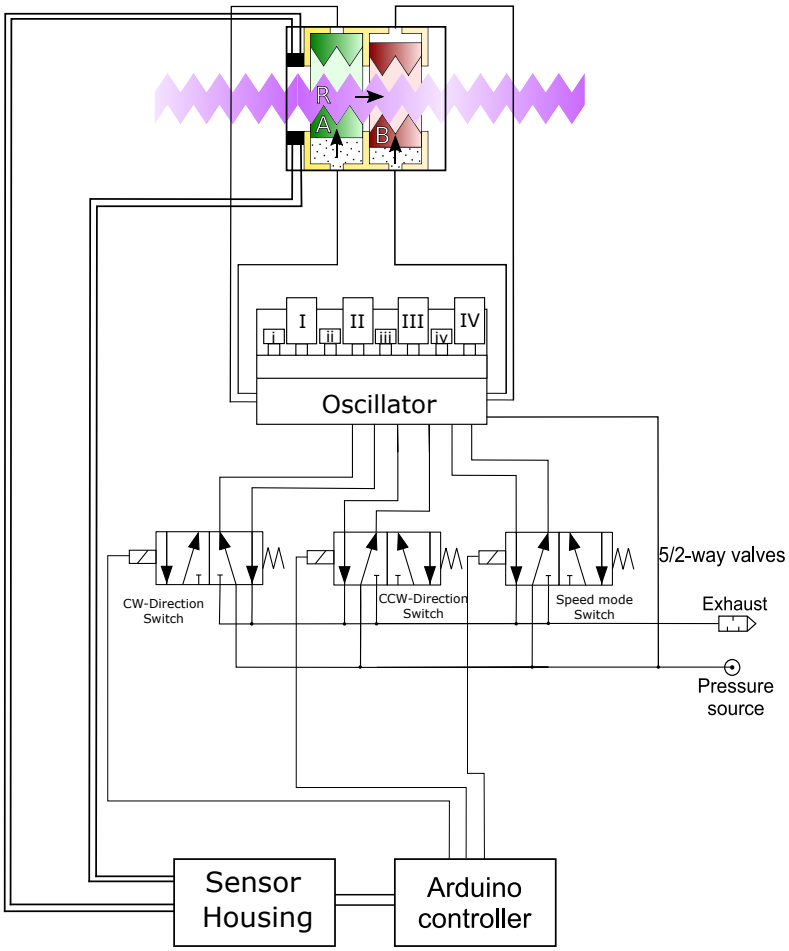

Figure 3.13: Schematic for controlling Pneumatic stepper motor with Oscillator and Solenoid valves.

pressurized air or the small Roman numerics. Due to the difference in the volume of the chambers, the time requires to fill them would be different which would subsequently decide the time delay of switching to the next sequence.

The controller compares the feedback steps to the input distance, if the input distance is less than zero, the controller switches the direction of the stepper motor by sending a signal to the solenoid responsible for generating the quadrature signal of that direction. Accordingly, the stepper motor is given signal for that direction until the stepper motor has taken the number of steps required to complete the input distance. In the case of overshoot, the controller changes the direction of the quadrature signal by switching the solenoid channel.

3.5 Experiments

This section describes the experiments conducted to investigate the performance of different control strategies developed using the integration of optical encoder with the MR safe pneumatic stepper motor and finally to evaluate the performance of the oscillator system integrated with the smart pneumatic stepper motor.

The experimental setup used is quite straight forward, the stepper motor is commanded to move 100 steps and the distance travelled vs time is plotted for each control strategy developed. The experiments performed was used to evaluate the performance of the smart stepper motor with solenoid valves as the controller manifold as well as with the new proposed controller manifold - Oscillator system. All the

systems are then compared to the previous stepper motor which uses a simple feedforward method and long pneumatic lines connected to a pair of 5/2-way solenoid valves.

3.5.1 Motivation

The different experiments that are performed using the same test setup had different inferences.

Experiment- 1 is performed with the smart stepper motor, i.e. the stepper motor integrated with the optical encoder in order to see how much the working region has increased with just using a simple control algorithm i.e. "Error Correction Strategy". The working region can be defined as the combination of two parameters, step-frequency and source pressure at which the stepper motor makes no mistake or is able to complete the commanded steps. For the feedforward control method, if the stepper motor makes a mistake it would be unable to account for the missing steps, this can be solved either by increasing the source pressure or by decreasing the step-frequency the right combination of these parameters was found and shown in the plot.

Experiment-2 is done to get a benchmark of the feedforward method using different pneumatic lines. Two different pneumatic lines were used, 2 m and 5 m tubes and the working region of the stepper motor were found for both cases.

Experiment- 3 is done to find the distance travelled vs time plot of the Oscillator at different source pressure. This also gives us the performance of the smart stepper motor at 4 bar pressure which is the standard working pressure for the robotic system this actuator is used for.

Experiment- 4, the final experiment was done to compare all the control strategies developed, i.e. Error Correction, Adaptive Frequency strategy and the performance of the oscillator system. This was compared with the feedforward control strategy which was used previously by the MR safe stepper motor and the different robotic system.

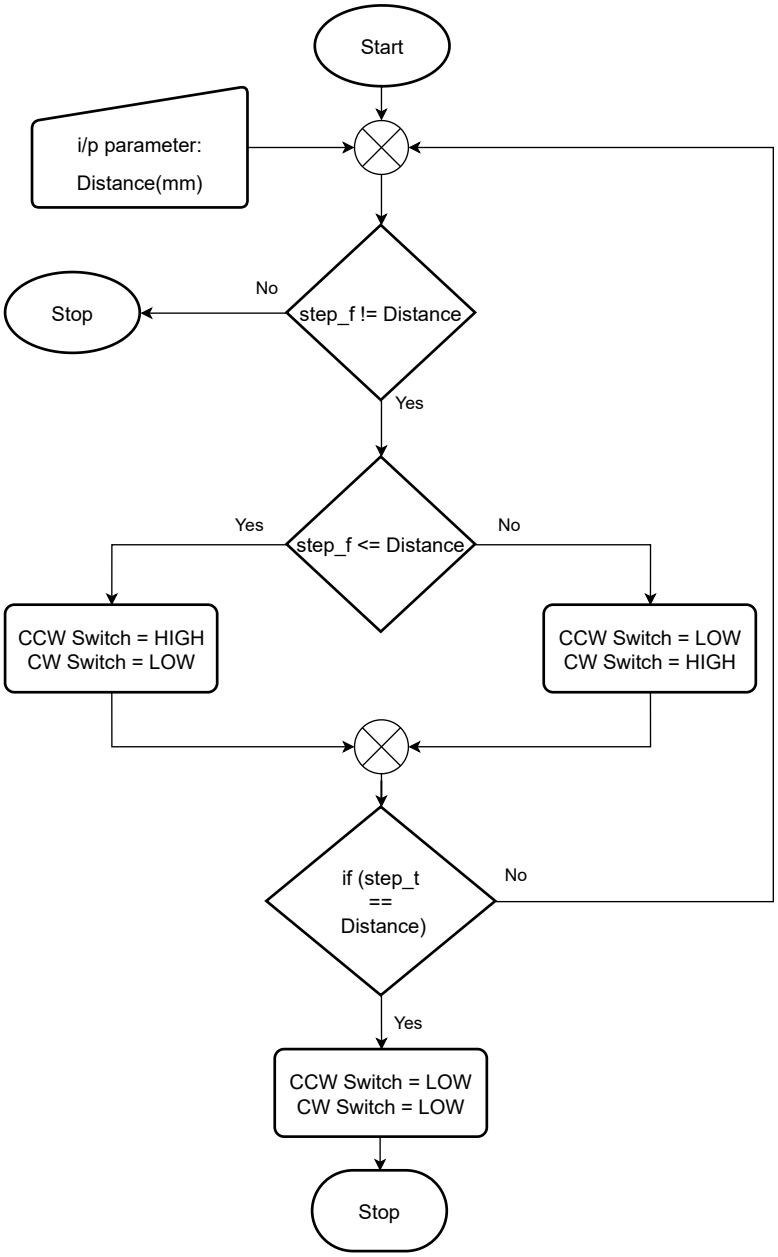

Figure 3.14: Control strategy for Pneumatic Oscillator system

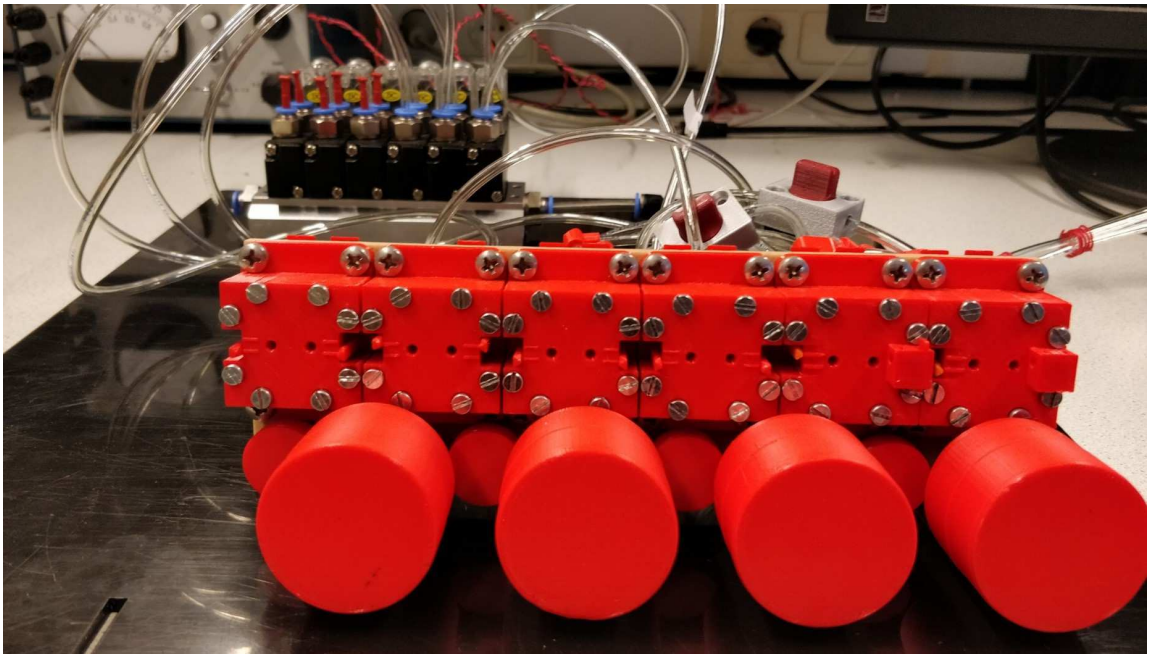

Figure 3.15: Oscillator integrated with solenoid and stepper motor

Chapter 4

Results

This section shows the results of the different experiments performed. And in the last section of this chapter, the results are discussed.

4.1 Working Region of Pneumatic Stepper Motor

The robotic system needs to be MRI safe so, in order to run the robot using a solenoid, 5 m pneumatic lines would be used, so the major focus for the feedback system was given to this case. This experiment was focused on the first strategy devised using the feedback system, i.e., Error Correction strategy. The plot shown in fig. 4.1 shows the increase in the working region using the feedback system.

The plot represents the benefit of using a Feedback system as it shows the increase in the working region or the combination of pressure and stepping frequency which can be used for the stepper motor to complete the given number of steps. The presence of a feedback system allows the stepper motor to work at a higher step frequency, which increases the speed of the stepper motor by 33%.

The result shows the working region of the pneumatic system for 2 m and 5 m pneumatic line. The plot, fig. 4.2 shows the combination of Pressure and stepping frequency under which the stepper motor will work without making any error for a pneumatic tube length of 2 m and 5 m. Longer tube has higher pressure drop which results in reducing the flow rate $\dot{Q}$, due to which it takes a longer duration of time to fill the chamber and the pneumatic tubes which in turn moves the stepper motor ahead. From the plot, it is clear that there is a huge effect of the pneumatic tube length on the performance of the stepper motor. The next experiment is showcasing the new oscillator system which would reduce the pneumatic lines from 5 m to 1 m.

4.2 Pneumatic Oscillator

The experiment was done to find the working condition and the average step frequency of the stepper motor at different pressure. The stepper motor was commanded to move 100 mm and using the optical encoder the time taken to complete the input step was recorded and is shown in fig. 4.3.

From the figure one can see that for pressure less than 2.5 bar, the stepper motor was making mistake and slipping. This shows that the system working condition is more than 2 bar. From the figure, it is also clear that after 4bar, the Oscillator does not show any improvement in step frequency. The average velocity plot fig. 4.4 shows that at 4 bar and 4.5 bar working pressure the stepper motor has saturated its speed and it can't increase its velocity. Also, the oscillator is not able to move the stepper motor below 1.5 bar pressure. From fig. 4.3, the average velocity for the oscillator system working at different pressure was found and is

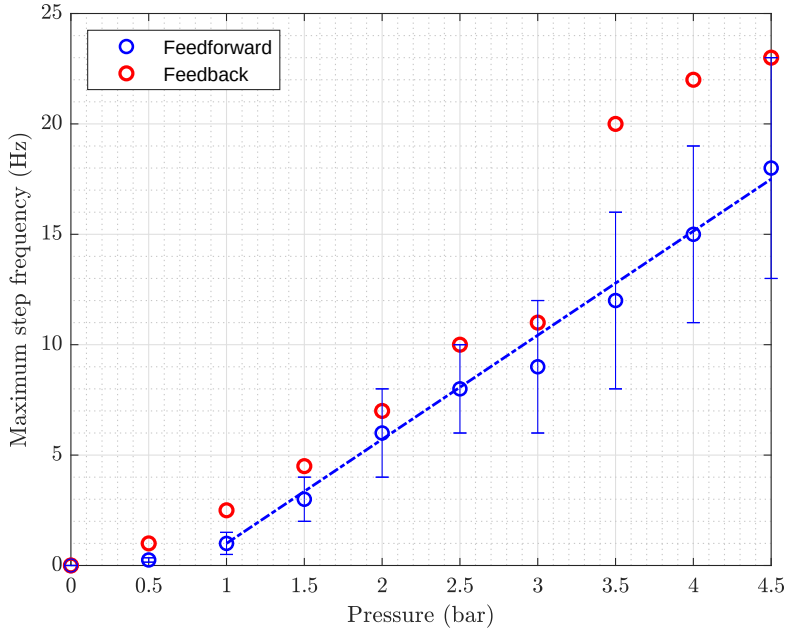

Figure 4.1: **Working region of stepper motor with and without feedback:** Using feedback strategies has increased the working region of the stepper motor by a factor of 2 below 1 bar and by a factor of 1.5 above 3.5 bar, but only has minor effect between 1 to 3.5 bar.

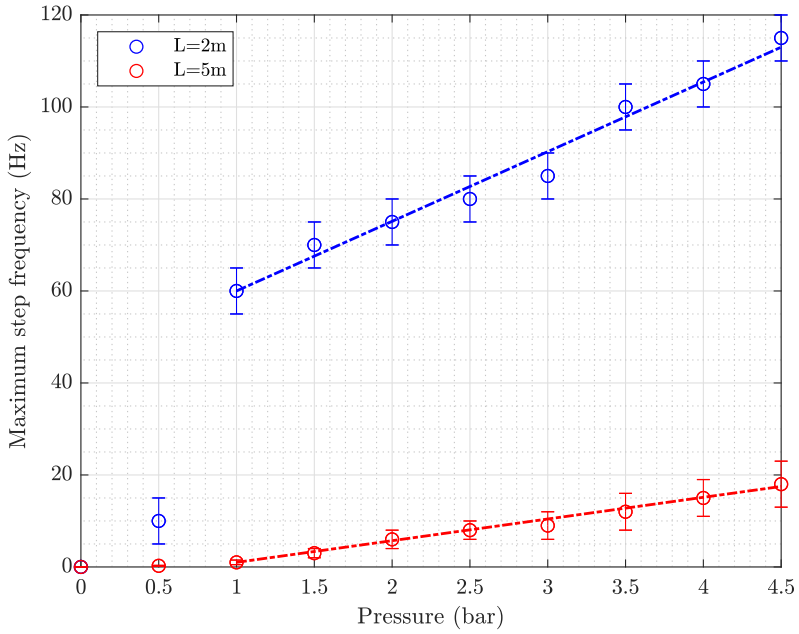

Figure 4.2: **Working region of stepper motor for 2 m and 5 m pneumatic line without feedback:** Plot shows a linear relation for both 2 m and 5 m line above 1 bar pressure. The difference between the maximum step frequency for 2 m and 5 m line after 1 bar pressure is on an average greater than by a factor of 10.

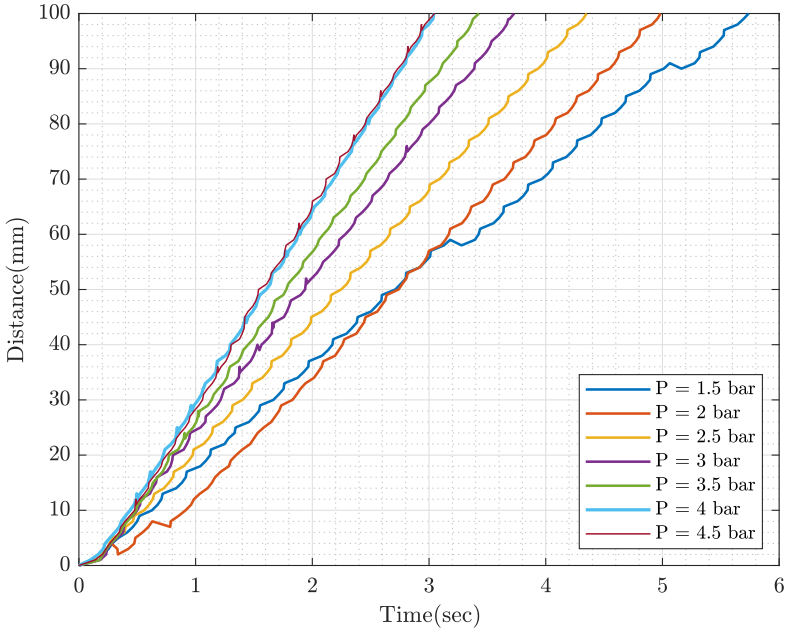

Figure 4.3: **Distance travelled vs time plot for oscillator system at different pressure values:** Plot shows the minimum pressure required to run the stepper motor without slipping which is **2.5 bar** and after **4 bar** increasing pressure does not yield better performance.

represented in the next plot, fig. 4.4.

4.3 Comparison of Different Control Strategies

In order to test the performance of the stepper motor with and without feedback, and the two control strategy developed which are "Error Correction strategy" and "Adaptive frequency strategy", the stepper motor was commanded to move 100 steps at 4 bar pressure same as the Oscillator system. Different readings are taken for the different strategy at different step frequency for Feedforward control and Error Correction strategy were taken and the results which are the fastest and made no error are taken for comparison. The plot shown is the distance travelled vs time (fig. 4.5) of each method.

4.4 Discussion

This section discusses the different experiment performed and the interpretation of the found results.

In section 4.1, experiments were done in which the stepper motor was programmed to move 100 steps and at different combination of step frequency and input pressure, the performance of the stepper motor was observed and noted in which it made no mistake. This was done for both 2 m and 5 m pneumatic lines. This was done in order to get a baseline of the performance of the stepper motor without a feedback system and to find the effect of the pneumatic line on the performance of the stepper motor.

The result shown in fig. 4.2, shows that there is a linear relation between the rise in step frequency and pressure above 1 bar pressure. There is a spike in the maximum step frequency achieved after 0.5 bar which is due to the minimum critical force required by the piston to move on the rack. Also at lower pressure, the flow rate is also reduced due to which the stepper motor requires more time to pressurize the chamber. The difference between the maximum step frequency achieved by 2 m and 5 m pneumatic line is because

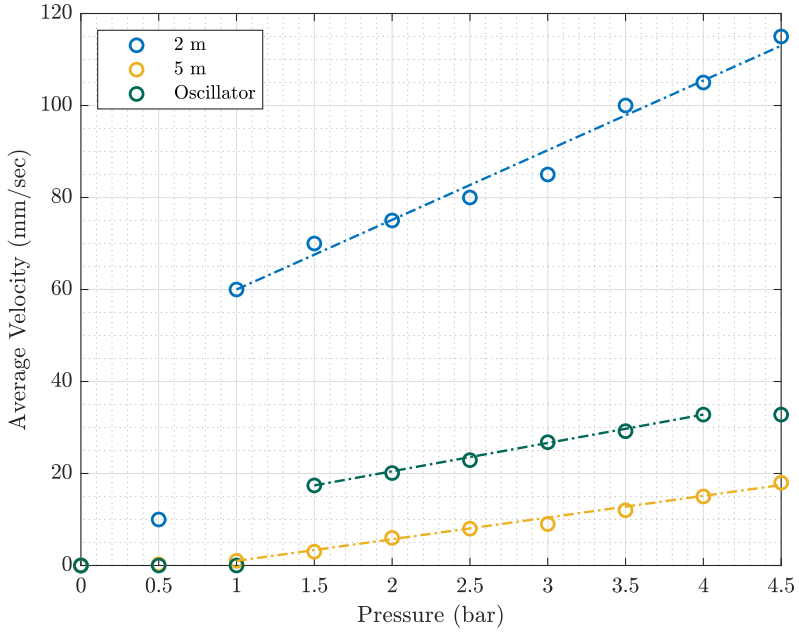

Figure 4.4: **Average velocity of Oscillator at different Pressure value:** Plot shows the average velocity of the stepper motor when using Pneumatic Oscillator to operate. The saturation of the system after 4 bar can be seen and the minimum pressure required to run the stepper motor using the Pneumatic oscillator system is 1.5 bar. There is a linear relation between average velocity and pressure for the oscillator system. The plot also shows the average velocity achieved by solenoid system using 2 m and 5 m pneumatic lines.

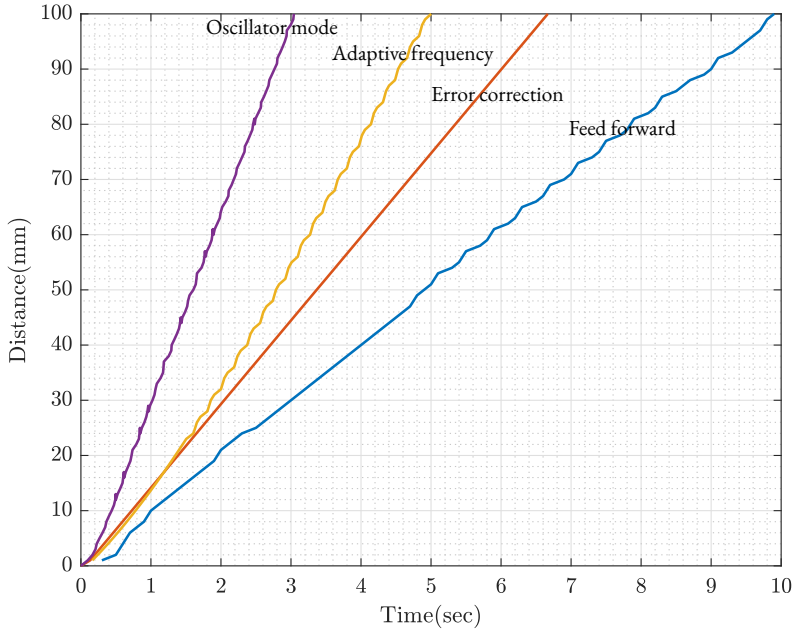

Figure 4.5: **Comparison of different systems:** Plot compares the performance of all the systems investigated in this document at 4 bar pressure. **Oscillator system** is faster by a factor of 3.3, followed by the **adaptive frequency strategy** with a factor of 2 and finally, the **error correction strategy** by a factor of 1.5 with respect to the **feedforward method** as a baseline. From the relation between Adaptive frequency and Error Correction it is clear that there is no advantage in using adaptive frequency strategy for distances less than 2 cm.

longer tubes have a higher pressure drop which results in a reduction of flow rate. The difference between their rise can be found from the slope of the linear fit. The slope for 2 m and 5 m pneumatic lines are $y_{2\,\mathrm{m}} = 15.143x_{2\,\mathrm{m}}$ and $y_{5\,\mathrm{m}} = 4.857x_{5\,\mathrm{m}}$. The slope for a 2 m Pneumatic tube is around 3 times greater than that for a 5 m pneumatic tube. The difference in the slope is due to the relation between flow rate ($\dot{Q}$) and pneumatic lines. The flow rate and input pressure define the duration required to fill the chamber which in turn pushes the piston to move on the rack.

Now that there is a baseline, we can compare the increase in the working region of the Pneumatic stepper motor integrated with an optical encoder. The next experiment was done to find how a simple error correction strategy can increase the overall working region of the stepper motor. Fig. 4.1, shows that using a simple feedback strategy increased the working region of the stepper motor by 50% below 1 bar and by 30% above 3.5 bar. There was a very minor effect in increasing the working region between 1 to 3.5 bar, which can e explained by the same pressure and flow rate relation. For pressure less than 3.5 bar, the flow rate was not enough for higher step frequency to move the rack and due to less pressure, there was not enough force. And the spike at 0.5 bar pressure is due to fulfilling the minimum pressure/force criteria.

The next experiment (section 4.2) done was to find the working conditions and average step frequency of the pneumatic stepper motor at different pressure using a pneumatic oscillator, which is a replacement of the solenoid valves that were used as the valve manifold. The stepper motor was commanded to move 100 mm and using the encoder the distance travelled vs time plot was made. From the fig. 4.3, it is clear that for pressure less than 2.5 bar, the stepper motor was making mistake and slipping. This shows that the systems working condition is more than 2 bar and after 4 bar pressure, the oscillator does not yield any improvement in average step frequency, the current version of the system gets saturated at 4 bar pressure. From fig. 4.4, the saturation of the Oscillator system after 4 bar can be seen and the minimum pressure required to run the stepper motor using the Oscillator system is 1.5 bar. The oscillator also has a linear relation between the average velocity achieved at different pressure. This is due to the fact that the pneumatic lines connected to the stepper motor using the oscillator are only 1 m. Due to the small pneumatic lines, the flow rate at the pneumatic lines is higher as compared to that of the 5 m pneumatic line using solenoid as valve manifold. The average velocity achieved by this system is faster than that from the 5 m pneumatic lines but still, it is less than that of the 2 m pneumatic line. This is due to the fact that the oscillator is a complete mechanical system and does not have a high response time as compared to an electrical solenoid system.

The final experiment done was to compare the different control strategies developed or investigated in this thesis. The stepper motor was commanded to move 100 steps at 4 bar pressure and the performance of different control strategies were recorded using the integrated optical encoder which is shown in fig. 4.5. Traditionally feed-forward method was used to control the stepper motor, which limits the maximum step frequency to 10 Hz due to which the stepper motor completed the commanded steps in 10 second. This was used as the baseline to compare the different methods investigated in this thesis. *The oscillator system* output is the fastest system with 3 sec to complete the commanded steps, after which comes the adaptive control method which uses solenoid and 5 m pneumatic line, similar conditions were given for the other methods i.e. Error correction(requires new data) and feed-forward control was also tested with 5 m pneumatic line. The *adaptive frequency strategy* took 5 seconds to complete the commanded steps and *error correction strategy* took 6.6 seconds. Which lead to the oscillator system being faster by a factor of 3.3 times, adaptive frequency by a factor of 2 times and error correction by 1.5 times.

From this, we can conclude that pneumatic stepper motor with feedback incorporated in them can run the stepper motor twice as fast without a feedback system. The addition of the feedback system allows the implementation of different type of control strategy which would allow the stepper motor to become more robust to the non-linear conditions of the pneumatic system.

The Error Correction strategy also improved the working region of the stepper motor for lower pressure and stepping frequency but was not enough for the case of 4bar pressure and higher stepping frequency.

Upon further investigating the performance of the Error Correction strategy, it is found that it is not able to make correction at higher step frequency when operating at 4 bar pressure. Once it makes a mistake it gets stuck in that step as it is not able to generate enough pressure inside the chamber to move on the rack. After performing several experiments and recording data using the optical encoder, it was observed that at 4 bar for higher stepping frequency (more than 10 Hz) the stepper motor was not able to move at the beginning which was caused because the chambers inside the stepper motor were not pressurised enough to push the rack. The adaptive frequency strategy starts with a lower stepping frequency and then keep on increasing its step frequency exponentially which counters this problem. The adaptive frequency strategy can be tuned so that it can adapt to the change in the flow rate of the pneumatic signal. This will allow the stepper motor to become as fast as possible for the given conditions without investigating in depth. And finally, the optical encoder allowed easier integration of the oscillator with the smart pneumatic stepper motor, otherwise controlling the stepper motor using just the oscillator would have been very complicated.

Table 4.1: **Complexity analysis:** The smart pneumatic stepper motor with oscillator system is a highly complex setup in comparison to a simple pneumatic stepper motor without feedback.

Type of component		No of components:		
		Pneumatic Stepper motor	Smart Pneumatic Stepper motor	Smart Pneumatic stepper motor with Oscillator
Electrical component	Solenoid	2	2	3
	LED	0	2	2
	Photointerrupters	0	2	2
Additional mechanical component	Mechanical Oscillator	0	0	1
	Optical wire	0	4	4
No of pins required to run one stepper motor		2	4 (2 interrupt pins)	5 (2 interrupt pins)

The complexity table was made to quantify the advantage or disadvantage of the two systems designed with the traditional pneumatic stepper motor system. The different components of each system are listed here and from the table 4.1, it is clear that the smart pneumatic stepper motor with Oscillator is a very complex system. After adding the extra 9 components in comparison to the standard pneumatic stepper motor, the oscillator system is able to perform faster by a factor of 3.3 times. Another advantage of the oscillator system is that the force output is greater than the previous system even after achieving a higher step frequency. The low average velocity in comparison to the solenoid system using a 2 m pneumatic line is due to the fact that the oscillator system is a completely MR safe mechanical system due to which the response time for switching state is not as high as that of the electrical solenoid.

Chapter 5

Conclusion

This chapter explains the conclusion of the work done throughout the thesis and the future recommendations that can improve the performance of the system investigated.

5.1 Conclusion

To conclude this thesis, it will be assessed to what extent the goal described in chapter 1 is met. The overall goal of this thesis was to design and evaluate a smart controller for MR safe pneumatic stepper motor and a possibility of integration with the pneumatic oscillator. Therefore, a distance vs time profile of a traditional and smart pneumatic stepper motor was compared. Also, the use of a pneumatic valve manifold and oscillator to drive the smart pneumatic stepper motor was investigated.

To this extent, the first research goal was to analyse the use of optical encoder as a feedback mechanism. Once the MR safe optical was designed, different control strategies were compared against the feed-forward control strategy as a baseline. By using a simple control strategy involving a feedback system i.e. error correction method, the stepper motor showed an improvement in its working region by a factor of 2 below 1 bar and for pressure above 3.5 bar by a factor of 1.5. For pressure between 1 and 3.5 bar, it showed very little improvement. Upon further analysing the working of the stepper motor, the adaptive frequency strategy was developed which showed an improvement by a factor of 2. Further, it is also observed that for distances longer than 2 cm the adaptive frequency strategy works best and for distances smaller than 2 cm the error control strategy shows better results.

The second research goal was to compare the performance of a traditional long-distance valve with the novel pneumatic oscillator. Using the traditional solenoid and 2 m pneumatic lines, after 1 bar working pressure the stepper motor was able to achieve a maximum step frequency greater than the 5 m pneumatic line by a factor of 10. The solenoid valves were used to integrate the pneumatic oscillator with the stepper motor. Upon this integration, it was observed that the performance of this combined system was improved by a factor of 3.3 with respect to the feed-forward method with long traditional solenoid valves as a baseline. The minimum pressure to drive the stepper motor using an oscillator is identified as 1.5 bar, whereas no further improvement in performance was observed beyond 4 bar. After analysing the different components of the three systems, it is clear that a smart pneumatic stepper motor with an oscillator system is a highly complex setup in comparison to that of a traditional stepper motor system.

To conclude the overall work done in this thesis, an MR safe optical encoder was designed and evaluated, which was further integrated with the pneumatic stepper motor. This combined system is referred to as a smart pneumatic stepper motor. Further, this smart pneumatic stepper motor lends itself to facilitate automatic calibration and implementation of various control strategies. This further improved the performance of the overall system by means of feedback control, theoretically increases the safety of the

system and easy integration with a pneumatic oscillator system.

5.2 Future Recommendations

This section highlights the future work that can be done to further improve the smart pneumatics stepper motor and the integration with the oscillator system.

The main limitation of the optical encoder which is developed is that it has a resolution of 1 mm which is similar to the step resolution of the motor. This can be improved further by changing the dimension of slits and using a thinner optical cable.

Due to the presence of a feedback system, more control strategies can be developed or tested.

Using another Arduino for keeping track of all the position of the stepper motor and serial communication between the observer and the controller would improve the code performance.

Adaptive frequency strategy can be improved by further tuning the gain values and creating a calibration protocol for this control strategy.

The main limitation of the oscillator right now is that it doesn't show any improvement in the average velocity of the stepper motor after 4 bar pressure, this can be improved by tweaking the architecture of the oscillator specifically the air tanks which is used for creating the delay.

Acknowledgements

At the end of this thesis, I would like to thank all the people without whom I would not have been able to complete my assignment. Although it is just my name on the cover, many people have contributed to this research in their particular way, and for that, I want to give them special thanks.

Firstly, to my supervisor dr. V. Groenhuis, and my chair prof. dr. ir. L. Abelmann, without their guidance this assignments outlook would have been very different. I am highly grateful for their quick and active support whenever I was stuck or got confused and to help me think in a new way which made me a better researcher.

And at the end, I would like to take a moment to thank my friends and family for providing me with their moral support during the thesis. Their support was also the reason why during the COVID-19 lockdown I was able to maintain my composure.

Bibliography

[1] V. Groenhuis and S. Stramigioli. Rapid prototyping high-performance mr safe pneumatic stepper motors. *IEEE/ASME Transactions on Mechatronics*, 23(4):1843–1853, Aug 2018.

[2] V. Groenhuis. Pneumatic oscllator schematics. Technical report, Robotics and Mechatronics, University of Twente, Control Laboratory, EL/RAM, Faculty of Electrical Engineering, Mathematics & Computer Science, University of Twente, P.O. Box 217, 7500 AE Enschede, The Netherlands, March, 2021. Internal document (unpublished).

[3] Sandra B. Brennan. Breast magnetic resonance imaging for the interventionalist: Magnetic resonance imaging–guided vacuum-assisted breast biopsy. *Techniques in Vascular and Interventional Radiology*, 17(1):40–48, 2014. Breast Interventions.

[4] Marie-Claude Chevrier, Julie David, Mona El Khoury, Lucie Lalonde, Maude Labelle, and Isabelle Trop. Breast biopsies under magnetic resonance imaging guidance: Challenges of an essential but imperfect technique. *Current Problems in Diagnostic Radiology*, 45(3):193–204, 2016.

[5] Vincent Groenhuis, Françoise Siepel, Jeroen Veltman, JK Zandwijk, and Stefano Stramigioli. Stormram 4: An mr safe robotic system for breast biopsy. *Annals of Biomedical Engineering*, 46, 05 2018.

[6] "Vincent Groenhuis, Françoise Jeanette Siepel, and Stefano Stramigioli". *"Sunram 5: A Magnetic Resonance-Safe Robotic System for Breast Biopsy, Driven by Pneumatic Stepper Motors"*, pages "375–396". "Elsevier", "1st" edition, sep "2019".

[7] D. Stoianovici, A. Patriciu, D. Petrisor, D. Mazilu, and L. Kavoussi. A new type of motor: Pneumatic step motor. *IEEE/ASME Transactions on Mechatronics*, 12(1):98–106, 2007.

[8] Joyce Bomers, Dennis Bosboom, Gerrit Tigelaar, Jan Sabisch, J. Fütterer, and D. Yakar. Feasibility of a 2 generation mr-compatible manipulator for transrectal prostate biopsy guidance. *European Radiology*, 27, 07 2016.

[9] Gaurav Bhide. Evaluation of the sunram 5 for performing a full clinical in-situ breast biopsy procedure, August 2020.

[10] H. Su, I. I. Iordachita, J. Tokuda, N. Hata, X. Liu, R. Seifabadi, S. Xu, B. Wood, and G. S. Fischer. Fiber-optic force sensors for mri-guided interventions and rehabilitation: A review. *IEEE Sensors Journal*, 17(7):1952–1963, 2017.

[11] Fabrizio Taffoni, Domenico Formica, Paola Saccomandi, Giovanni Di Pino, and Emiliano Schena. Optical fiber-based mr-compatible sensors for medical applications: An overview. *Sensors*, 13(10):14105–14120, 2013.

[12] Sang-Hoon Kim. Chapter 9 - speed estimation and sensorless control of alternating current motors. In Sang-Hoon Kim, editor, *Electric Motor Control*, pages 373–388. Elsevier, 2017.

[13] Ciprian-Radu Rad and Olimpiu Hancu. An improved nonlinear modelling and identification methodology of a servo-pneumatic actuating system with complex internal design for high-accuracy motion control applications. *Simulation Modelling Practice and Theory*, 75:29–47, 2017.

[14] "Vincent Groenhuis, Françoise Jeanette Siepel, and Stefano Stramigioli". "dual-speed mr safe pneumatic stepper motors". In *"Dual-Speed MR Safe Pneumatic Stepper Motors"*, jun "2018". "Robotics: Science and Systems 2018, RSS 2018 ; Conference date: 26-06-2018 Through 30-06-2018".

[15] N. Sariff and Norlida Buniyamin. An overview of autonomous mobile robot path planning algorithms. In *An Overview of Autonomous Mobile Robot Path Planning Algorithms*, pages 183 – 188, 07 2006.

[16] Yaser Maddahi, Kourosh Zareinia, Boguslaw Tomanek, and Garnette R Sutherland. Challenges in developing a magnetic resonance–compatible haptic hand-controller for neurosurgical training. *Proceedings of the Institution of Mechanical Engineers, Part H: Journal of Engineering in Medicine*, 232(12):1148–1167, 2018.

[17] Soňa Kontárová, Radek Přikryl, Veronika Melcova, Přemysl Menčík, Matyáš Horálek, Silvestr Figalla, Roderik Plavec, Jozef Feranc, Jiří Sadílek, and Aneta Pospíšilová. Printability, mechanical and thermal properties of poly(3-hydroxybutyrate)-poly(lactic acid)-plasticizer blends for three-dimensional (3d) printing. *Materials*, 13:4736, 10 2020.

[18] M. Belgharbi, Sylvie Sesmat, Serge Scavarda, and Daniel Thomasset. Analytical model of the flow stage of a pneumatic servo-distributor for simulation an nonlinear control. In *SICFP*, volume 2, pages 847–860, Tampere, Finland, May 1999.

[19] S. B. Kesner and R. D. Howe. Design principles for rapid prototyping forces sensors using 3-d printing. *IEEE/ASME Transactions on Mechatronics*, 16(5):866–870, 2011.

[20] Yusuf Mert Senturk and Volkan Patoglu. Mri-visact: a bowden-cable-driven mri-compatible series viscoelastic actuator. *Transactions of the Institute of Measurement and Control*, 40(8):2440–2453, 2018.

[21] Reza Monfaredi, Kevin Cleary, and Karun Sharma. Mri robots for needle-based interventions: Systems and technology. *Annals of Biomedical Engineering*, 46, 06 2018.

[22] Garry Berkovic and Ehud Shafir. Optical methods for distance and displacement measurements. *Adv. Opt. Photon.*, 4(4):441–471, Dec 2012.

[23] Yeming Zhang, Ke Li, Shaoliang Wei, and Geng Wang. Pneumatic rotary actuator position servo system based on ade-pd control. *Applied Sciences*, 8:406, 03 2018.

[24] N. Hendrich, F. Wasserfall, and J. Zhang. 3d printed low-cost force-torque sensors. *IEEE Access*, 8:140569–140585, 2020.

[25] C. Saranya, K. Koteswara Rao, Manju Unnikrishnan, Dr. V. Brinda, V.R. Lalithambika, and M.V. Dhekane. Real time evaluation of grid based path planning algorithms: A comparative study. *IFAC Proceedings Volumes*, 47(1):766–772, 2014. 3rd International Conference on Advances in Control and Optimization of Dynamical Systems (2014).

[26] Alessandro "Gasparetto, Paolo Boscariol, Albano Lanzutti, and Renato" Vidoni. *"Path Planning and Trajectory Planning Algorithms: A General Overview"*, pages "3–27". "Springer International Publishing", "Cham", "2015".

[27] Hao Su, Gang Li, and Gregory S. Fischer. *SENSORS, ACTUATORS, AND ROBOTS FOR MRI-GUIDED SURGERY AND INTERVENTIONS*, chapter Chapter 8, pages 201–231. Encyclopedia of Medical Robotics.

[28] F. Shellock and A. Spinazzi. Mri safety update 2008: part 2, screening patients for mri. *AJR. American journal of roentgenology*, 191 4:1140–9, 2008.

[29] P. Tomei. Adaptive pd controller for robot manipulators. *IEEE Transactions on Robotics and Automation*, 7(4):565–570, 1991.

[30] Fabrizio Taffoni, Domenico Formica, Paola Saccomandi, Giovanni Di Pino, and Emiliano Schena. Optical fiber-based mr-compatible sensors for medical applications: An overview. *Sensors*, 13:14105–14120, 10 2013.